

2

MISCELLANEOUS PAPER GL-88-11

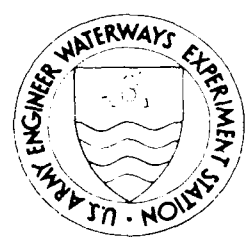
# ANALYSIS OF THE PILE LOAD TEST PROGRAM AT THE LOCK AND DAM 26 REPLACEMENT PROJECT

by

Larry M. Tucker, Jean-Louis Briaud

Civil Engineering Department  
Texas A&M University  
College Station, Texas 77843

DTIC FILE COPY



June 1988  
Final Report

Approved For Public Release. Distribution Unlimited

DTIC  
ELECTE  
JUL 05 1988  
S  
E  
D

Prepared for US Army Engineer District, St. Louis  
210 Tucker Boulevard, N., St. Louis, Missouri 63101-1986

Monitored by Geotechnical Laboratory  
US Army Engineer Waterways Experiment Station  
PO Box 631, Vicksburg, Mississippi 39180-0631

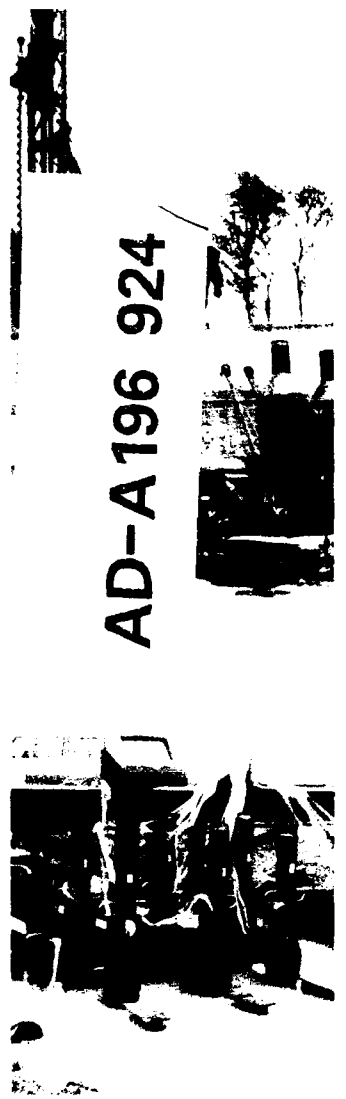
Under Contract No. DACW39-87-M-0752

88 7 01 040



US Army Corps  
of Engineers

AD-A196 924



REPORT DOCUMENTATION PAGE				Form Approved OMB No 0704 0188 Exp Date Jun 30 1986	
1a REPORT SECURITY CLASSIFICATION Unclassified		1b RESTRICTIVE MARKINGS			
2a SECURITY CLASSIFICATION AUTHORITY		3 DISTRIBUTION/AVAILABILITY OF REPORT Approved for public release; distribution unlimited			
2b DECLASSIFICATION/DOWNGRADING SCHEDULE					
4 PERFORMING ORGANIZATION REPORT NUMBER(S) Research Report 4690F		5 MONITORING ORGANIZATION REPORT NUMBER(S) Miscellaneous Paper GL-88-11			
6a NAME OF PERFORMING ORGANIZATION Texas A&M University	6b OFFICE SYMBOL (if applicable)	7a NAME OF MONITORING ORGANIZATION USAEWES Geotechnical Laboratory			
6c ADDRESS (City, State, and ZIP Code) College Station, TX 77843		7b ADDRESS (City, State, and ZIP Code) PO Box 631 Vicksburg, MS 39180-0631			
8a NAME OF FUNDING/SPONSORING ORGANIZATION US Army Engineer District, St. Louis	8b OFFICE SYMBOL (if applicable)	9 PROCUREMENT INSTRUMENT IDENTIFICATION NUMBER DACW39-87-M-9752			
8c ADDRESS (City, State, and ZIP Code) 210 Tucker Blvd. N. St Louis, MO 63101-1986		10 SOURCE OF FUNDING NUMBERS			
		PROGRAM ELEMENT NO.	PROJECT NO.	TASK NO.	WORK UNIT ACCESSION NO.
11 TITLE (Include Security Classification) Analysis of the Pile Load Test Program at the Lock and Dam 26 Replacement Project					
12 PERSONAL AUTHOR(S) Tucker, Larry M., Briaud, Jean-Louis					
13a TYPE OF REPORT Final report	13b TIME COVERED FROM _____ TO _____	14 DATE OF REPORT (Year, Month, Day) June 1988	15 PAGE COUNT 76		
16 SUPPLEMENTARY NOTATION Available from National Technical Information Service, 5285 Port Royal Road, Springfield, VA 22161.					
17 COSATI CODES			18 SUBJECT TERMS (Continue on reverse if necessary and identify by block number)		
FIELD	GROUP	SUB-GROUP			
			Piles Pile load tests In situ tests		
			Pressuremeter Cone penetrometer		
19 ABSTRACT (Continue on reverse if necessary and identify by block number) Prior to performing twenty-eight axial and two lateral load tests on piles at the Lock and Dam 26 project, an in situ test program was conducted. The program consisted of four cone penetration tests, twelve pressuremeter test borings, and four standard penetration test borings. Comparisons of pile capacity predictions were made for each of the in situ test methods. The initial study generated four reports and voluminous test data. This is a summary of those reports.					
20 DISTRIBUTION/AVAILABILITY OF ABSTRACT <input checked="" type="checkbox"/> UNCLASSIFIED/UNLIMITED <input type="checkbox"/> SAME AS RPT <input type="checkbox"/> DTIC USERS			21 ABSTRACT SECURITY CLASSIFICATION Unclassified		
22a NAME OF RESPONSIBLE INDIVIDUAL			22b TELEPHONE (Include Area Code)	22c OFFICE SYMBOL	

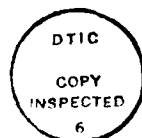
PREFACE

This report was funded by the US Army Engineer District, St. Louis (LMS) and prepared under Contract No. DACW39-87-M-0752 with the US Army Engineer Waterways Experiment Station (WES) during FY 87.

Mr. G. Britt Mitchell, Chief, Engineering Group, Soil Mechanics Division (SMD), Geotechnical Laboratory (GL), was Technical Monitor for the WES, under the supervision of Mr. C. L. McAnear, Chief, SMD, GL, and under the general supervision of Dr. W. F. Marcuson III, Chief, GL. The following individuals provided valuable contributions: from the LMS, P. J. Conroy, T. L. Crump, B. H. Moore, G. J. Postal, J. L. Schwenk, and T. F. Wolff; from the WES, R. F. Anderson, G. B. Mitchell, and J. B. Palmerton; from Texas A&M University (TAMU), T. E. Braswell, H. M. Coyle, L. G. Huff, W. D. Lawson, and M. A. Shihadeh. Messrs. Larry M. Tucker and Jean-Louis Briaud, TAMU, prepared the report.

COL Dwayne G. Lee, CE, is the Commander and Director. Dr. R. W. Whalin is Technical Director.

Accession For	
NTIS GRA&I	<input checked="" type="checkbox"/>
DTIC TAB	<input type="checkbox"/>
Unannounced	<input type="checkbox"/>
Justification	
By	
Distribution/	
Availability Codes	
Dist	Avail and/or Special
A-1	



## EXECUTIVE SUMMARY

A pile load test program was carried out for the new Lock and Dam 26 on the Mississippi River. Twenty-eight axial load tests and two lateral load tests were performed on H-piles and pipe piles. An in situ test program was conducted which consisted of four cone penetration test (CPT) soundings, twelve pressuremeter test (PMT) borings and four standard penetration test (SPT) borings.

The soil consisted of about 10 ft of alluvial deposits of poorly graded sands (SP) with some gravel having SPT blowcounts ranging from 15 to 40 blows per foot (bpf). Beneath this was about 45 ft of glacial deposits, predominantly of medium to coarse sand with gravel and cobbles, having SPT blowcounts ranging from 30 to 90 bpf with occasional refusal (>100 bpf). A hard clay layer with sand and gravel (glacial till, CL) about 3 ft thick lay between the sand and the limestone bedrock.

Overall, the sand layers had the following properties: dry unit weight - 110 pcf, water content - 19%, friction angle -  $35^{\circ}$ , average SPT blow count along the side of the piles - 30 bpf, average SPT blowcount at the pile tip - 65 bpf, average CPT sleeve friction - 0.8 tsf, average CPT point resistance - 225 tsf, average PMT net limit pressure along the side of the piles - 17 tsf, average PMT net limit pressure at the pile tip - 32 tsf. A statistical analysis of 13 SPT borings in the general test area showed an average horizontal coefficient of variation of 38%.

The axial load test program consisted of 13 tension and 9 compression tests of driven HP14x73 piles and one tension and one compression test on 12 in., 14 in. and 16 in. diameter pipe piles. The H-piles varied in length from 37 ft to 71 ft. The pipe piles varied in length

from 36 ft to 48 ft. The pipe piles were filled with sand during the tension tests and with concrete during the compression tests. Thirteen of the H-piles were driven vertically and eight were driven on a 1:2.5 batter to determine the effect of pile batter on axial capacity. Eleven of the H-piles were tested using the ASTM Standard procedure and eleven were tested using the ASTM Quick procedure to determine the effect of test procedure on pile capacity. The pipe piles were all driven vertically and tested using the ASTM Standard procedure.

The piles were all driven with an ICE 640 diesel pile driving hammer with a rated maximum energy of 40,000 ft-lbs. The average blow count for the last foot of penetration ranged from 9 to 38 bpf with an average of 25 bpf for the short piles which stopped in the soil above the bedrock, and from 63 to 81 bpf with an average of 74 bpf for the long piles driven to bedrock.

The ultimate capacity of the piles was defined as the load at a settlement equal to one-tenth of the pile diameter plus the elastic compression of the pile under this load. The stiffness of the pile is defined as the allowable load (assuming a factor of safety of 2) divided by the settlement at that load. Since the load-settlement curves are approximately linear up to this point the stiffness is simply the initial slope of the load-settlement curve.

The ultimate load for battered H-piles averaged 12% higher in tension and 25% lower in compression than comparable vertical H-piles. The initial stiffness of the battered H-piles averaged 74% higher in tension and 23% higher in compression than comparable vertical H-piles.

The ultimate load for Quick load tests on H-piles averaged 65% higher in tension and 43% higher in compression than Standard load tests

on comparable H-piles. The initial stiffness for Quick load tests on H-piles averaged 106% higher in tension and 5% lower in compression than Standard load tests on comparable H-piles.

The ultimate load for two H-piles with similar length, batter and load test procedure in the same pile group varied by 84%.

The settlements at working loads were small, however, the settlements of the H-piles averaged about three times those of the pipe piles in both tension and compression. The friction on the H-piles in tension averaged 24% lower than the friction of the pipe piles in tension. Both of these facts may be due to the larger displaced volume of the pipe piles, since they were driven closed-ended.

During driving residual stresses are locked into the pile as it tries to decompress after the hammer blow. The residual point loads on the H-piles averaged 26.5 tons which is 30% of the average point load measured in the compression tests.

Both dynamic capacity prediction methods, the Engineering News Formula and the Case method, gave predicted ultimate loads which were much lower than the ultimate loads measured in the load tests. A Wave Equation analysis showed that in order to match the ultimate loads in the load test a damping value of zero had to be used. In other words, a phenomenon similar to "setup" in clay may have taken place in this sand and gravel deposit. An analysis of the load transfer curves on four of the instrumented compression tests showed an average quake of 0.19 in. at the point and 0.11 in. on the side.

Eight static capacity methods were used to predict the pile capacities using the in situ tests results. The A.P.I. method was the best

SPT method for H-piles in tension and pipe piles in compression. The Briaud/Tucker method was the best SPT method for H-piles in compression and pipe piles in tension. The deRuiter/Beringen method was the best CPT method for H-piles in tension and compression, and the Laboratoire des Ponts et Chaussees method was the best CPT method for pipe piles in tension and compression. Based on an analysis of the predictions it was found that the H-piles capacities should be predicted using the perimeter of the enclosing rectangle for piles in tension. However, for compression capacity the H-piles should be assumed to be half-plugged, as this gives much better agreement with the measured point and side load distribution than either the full-plugged or unplugged assumptions.

The lateral load test program consisted of two 67 ft long H-piles which were jacked apart while measuring the deflection of each pile. The loading procedure included 25 cycles. Three methods were used to predict the monotonic pile response: the conventional P-y curves proposed by Reese et al., Broms' coefficient of subgrade reaction approach and Briaud et al. pressuremeter method. The conventional P-y curve prediction was very conservative. Broms' method matched the measured response well within the working load range. The pressuremeter method matched the entire load-deflection curve very well.

## TABLE OF CONTENTS

	Page
1. INTRODUCTION . . . . .	1
2. THE SITE AND THE SOIL . . . . .	2
2.1 The Test Site Location . . . . .	2
2.2 Soil Conditions . . . . .	2
2.3 Soil Variability . . . . .	15
3. THE AXIAL PILE LOAD TEST PROGRAM . . . . .	17
3.1 The Objectives . . . . .	17
3.2 The Piles . . . . .	17
3.3 The Load Test Procedures . . . . .	19
3.4 Definition of Measured Ultimate Load . . . . .	19
3.5 Load Test Results . . . . .	22
3.5.1 Ultimate Loads . . . . .	22
3.5.2 Residual Loads . . . . .	27
3.5.3 Shape of Load-Settlement Curve . . . . .	28
3.5.4 Effect of Pile Batter . . . . .	28
3.5.5 Effect of Load Test Procedure . . . . .	31
3.5.6 Variability Across Site . . . . .	32
3.6 Load Transfer Curves . . . . .	33
4. PREDICTED AXIAL PILE RESPONSE . . . . .	37
4.1 Pile Driving Analysis . . . . .	37
4.1.1 Pile Driving Analyzer . . . . .	37
4.1.2 Wave Equation Analysis . . . . .	37
4.1.3 Engineering News Formula . . . . .	42
4.2 Static Capacity Prediction Methods . . . . .	43
4.3 Comparison of Predicted and Measured Results . . . . .	44
4.4 Discussion of Results . . . . .	45
5. THE LATERAL LOAD TEST PROGRAM . . . . .	54
5.1 The Load Test Program . . . . .	54
5.2 The Prediction Methods . . . . .	54
5.3 Comparison of Predicted and Measured Results . . . . .	58
6. CONCLUSIONS . . . . .	60
7. REFERENCES . . . . .	62



## LIST OF TABLES

Number		Page
1	Horizontal Variability of SPT Data . . . . .	15
2	Description of Piles . . . . .	18
3	Pile Load Tests Results . . . . .	26
4	Load Distribution in Compression Tests . . . . .	26
5	Measured Residual Point Loads . . . . .	28
6	Comparison of Vertical and Battered Pile Response . . . . .	31
7	Comparison of Standard and Quick Test Procedures . . . . .	32
8	Measured Quake Values . . . . .	33
9	Pile Driving Analyzer Measurements . . . . .	38
10	Engineering News Formula Predictions . . . . .	42
11	Statistical Analysis of ENF Predictions . . . . .	43
12	Summary of Prediction Methods . . . . .	44
13	Summary of Soil Borings Used for Predictions . . . . .	44
14	Predicted and Measured Ultimate Loads in Tension . . . . .	45
15	Predicted and Measured Ultimate Loads in Compression . . . . .	46
16	Statistical Analysis of Tension Tests . . . . .	46
17	Statistical Analysis of Compression Tests on H-Piles - Plugged Case . . . . .	47
18	Statistical Analysis of Compression Tests on H-Piles - Unplugged Case . . . . .	47
19	Statistical Analysis of Compression Tests on H-Piles - Half-Plugged Case . . . . .	47
20	Statistical Analysis of Compression Tests of Pipe Piles . . . . .	48
21	Parameters Used for Reese et al. P-y Curves . . . . .	57

## LIST OF FIGURES

Number		Page
1	Location of Locks and Dam No. 26 Replacement . . . . .	3
2	Location of Pile Groups Within Phase 1 of Construction . . . . .	4
3	Soil Profile Across Test Site . . . . .	5
4	Gradation Band of Sieve Analysis Test Samples Obtained From SPT . . . . .	6
5	In Situ Tests Borings for Pile Group 1 . . . . .	8
6	In Situ Tests Borings for Pile Group 2 . . . . .	8
7	In Situ Tests Borings for Pile Group 3 . . . . .	9
8	Cone Penetrometer Test Soundings . . . . .	10
9	Standard Penetration Test Profiles . . . . .	11
10	Pressuremeter Parameter Profiles for Pile Group 1 . . . . .	12
11	Pressuremeter Parameter Profiles for Pile Group 2 . . . . .	13
12	Pressuremeter Parameter Profiles for Pile Group 3 . . . . .	14
13	Typical Driving Resistance Profile for Pile Terminating Above Rock . . . . .	20
14	Typical Driving Resistance Profile for Pile Driven to Rock . . . . .	21
15	Load Test Results for Compression Tests on H-Piles Driven to Rock . . . . .	23
16	Load Test Results for Tension Tests on H-Piles Driven to Rock . . . . .	23
17	Load Test Results for Compression Tests on H-Piles in Sand . . . . .	24
18	Load Test Results for Tension Tests on H-Piles in Sand . . . . .	24
19	Load Test Results for Compression Tests on Pipe Piles . . . . .	25
20	Load Test Results for Tension Tests on Pipe Piles . . . . .	25
21	Normalized Load-Settlement Curves for Compression Tests on H-Piles . . . . .	29
22	Normalized Load-Settlement Curves for Tension Tests on H-Piles . . . . .	29

	Page
23 Normalized Load-Settlement Curves for Compression Tests on Pipe Piles . . . . .	30
24 Normalized Load-Settlement Curves for Tension Tests on Pipe Piles . . . . .	30
25 Point Load Transfer Curves for H-Piles . . . . .	34
26 Average Side Load Transfer Curves for H-Piles . . . . .	35
27 Determination of 25% Secant Quake Values . . . . .	36
28 RUT Versus N for Pile 1-3A Using 25% Secant Quakes . . . . .	39
29 RUT Versus N for Pile 1-9 Using 25% Secant Quakes . . . . .	40
30 RUT Versus N for Pile 2-5 Using 25% Secant Quakes . . . . .	41
31 Predicted Versus Measured Ultimate Loads for H-Piles in Tension . . . . .	50
32 Predicted Versus Measured Ultimate Loads for Pipe Piles in Tension . . . . .	51
33 Predicted Versus Measured Ultimate Loads for H-Piles in Compression . . . . .	52
34 Predicted Versus Measured Ultimate Loads for Pipe Piles in Compression . . . . .	53
35 Lateral Load Test Setup . . . . .	55
36 Reese et al. P-y Curves in Sand . . . . .	56
37 Comparison of Predicted and Measured Lateral Deflections . . .	59

## 1. INTRODUCTION

This report is a summary of four reports analyzing the results of the load tests and capacity predictions based on in situ test methods for the pile load test program performed by the U.S. Army Corps of Engineers, St. Louis District, at the Locks and Dam 26 Replacement Project. The first report was an evaluation of in situ tests prediction methods for H-piles (Briaud, Huff, Tucker and Coyle, 1984). The second report evaluated three lateral load prediction methods (Briaud, rasuell and Tucker, 1984). The third report was a wave equation computer program analysis to determine the values of quake and damping for use in a gravelly sand (Briaud, Lawson and Tucker, 1984). The last report was a further evaluation of in situ tests prediction methods (Shihadeh, 1987). The load test program consisted of twenty-eight axial load tests which were performed to determine the effects of different loading procedures and pile batter on the compressive and tensile capacity of impact driven H-piles and pipe piles. Two lateral load tests were performed on driven H-piles.

The site and soil are characterized and the in situ test results are presented. The axial pile load test program is detailed and the load test results are compared to show the effect of load procedure, pile batter and site variation. The predicted axial pile response based on pile driving analysis and static capacity predictions from in situ tests results is presented. These predictions are compared to the measured response. The lateral load tests are described and the predicted and measured pile response are compared.

Conclusions are presented and recommendations are made for the use of in situ tests in pile capacity prediction.

## 2. THE SITE AND THE SOIL

### 2.1 The Test Site Location

The new Locks and Dam 26 is located on the Mississippi River at Alton, Illinois approximately 3 miles downstream from the old Locks and Dam 26 as shown on Figure 1. The project was constructed in three phases, the first of which consisted of six and one-half gatebays of the spillway and the stilling basin. The load test program was performed during this first phase. An area approximately 1000 ft by 800 ft was enclosed in cofferdams and the water evacuated. The load tests were performed in three groups located within the cofferdams as shown in Figure 2.

### 2.2 Soil Conditions

The overburden at the site may be divided into two categories: alluvial deposits, including Flood Plain Deposits, Recent Alluvium and Alluvial Outwash, and glacial deposits, including Wisconsinian Outwash, Illinoian Outwash and Illinoian Till (Conroy, 1985). The soil profile is shown in Figure 3. Before any pile driving took place, the river bottom within the cofferdams was lowered by excavating between 15 and 25 ft of alluvial deposits (see Figure 3). The alluvial deposits are generally poorly graded sand (SP) with some gravel, having standard penetration test (SPT) blow counts ranging from 15 to 40 blows per foot. The glacial deposits are outwash deposits ranging from clays to boulders, with a predominance of medium to coarse sand with gravel. The SPT blow counts ranged from 30 to 90 blows per foot with occasional refusal (>100 blows per foot). The bedrock below the glacial deposits is a hard limestone of Mississippian age (Conroy, 1985). A plot of grain size distributions for the soil is shown in Figure 4.

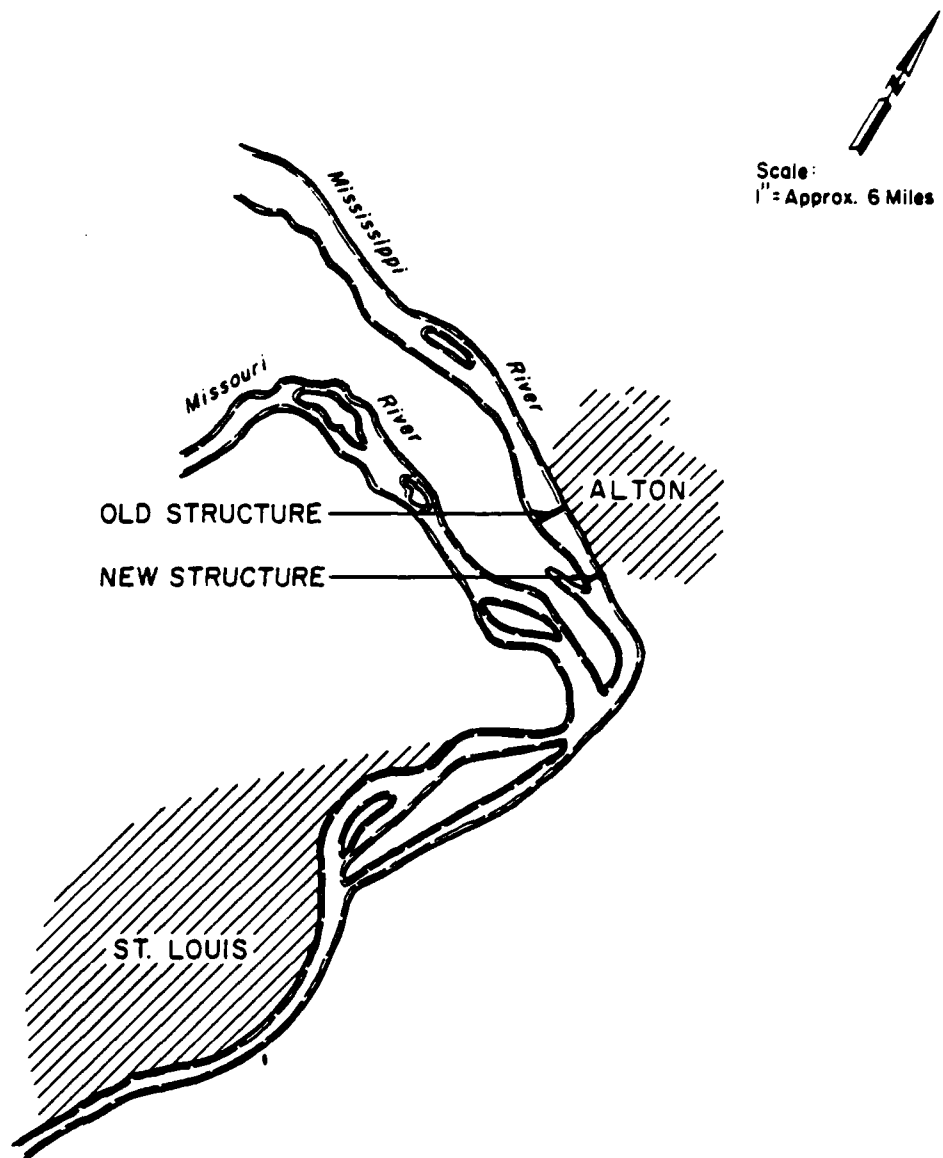


FIG. 1. Location of Locks and Dam No. 26 Replacement

Scale:  
1" = 200'

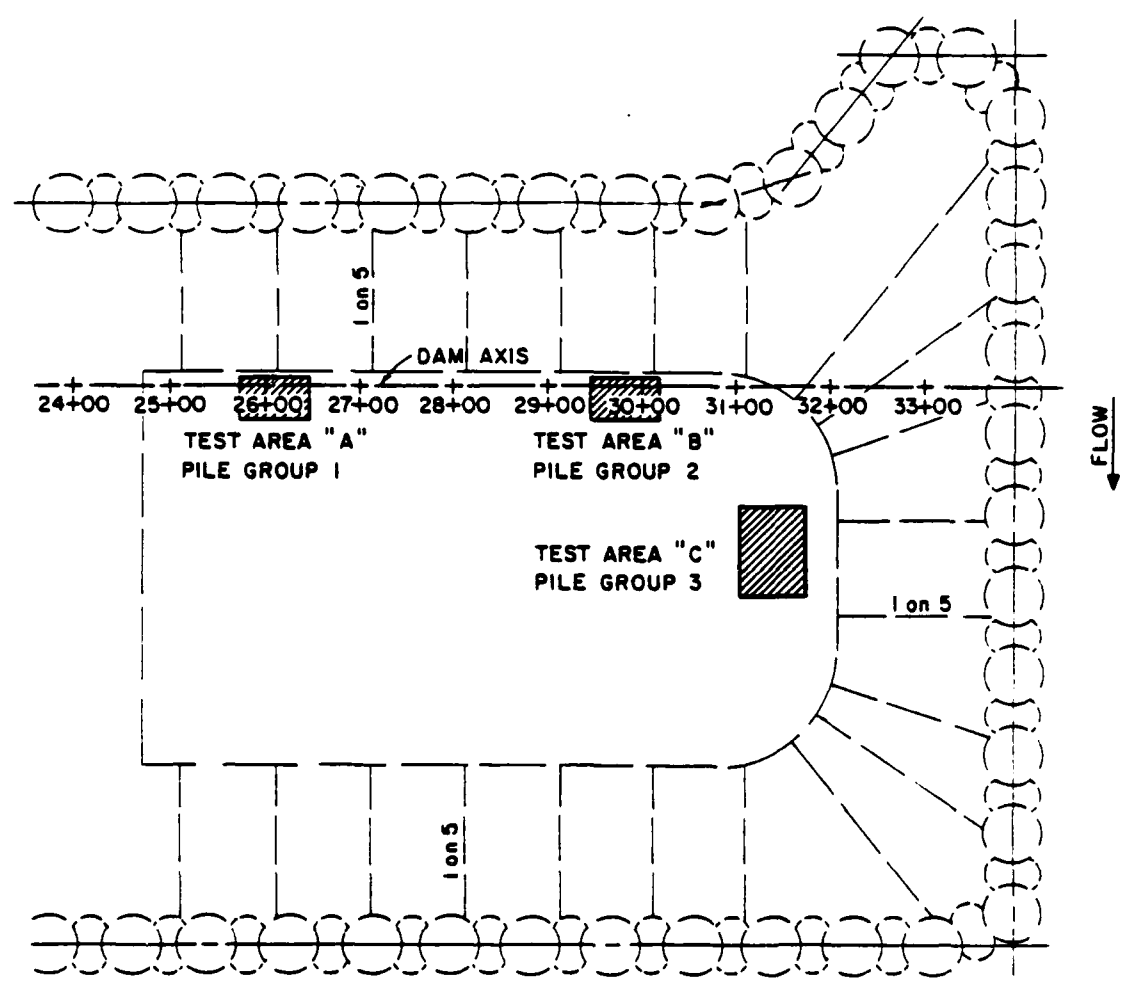
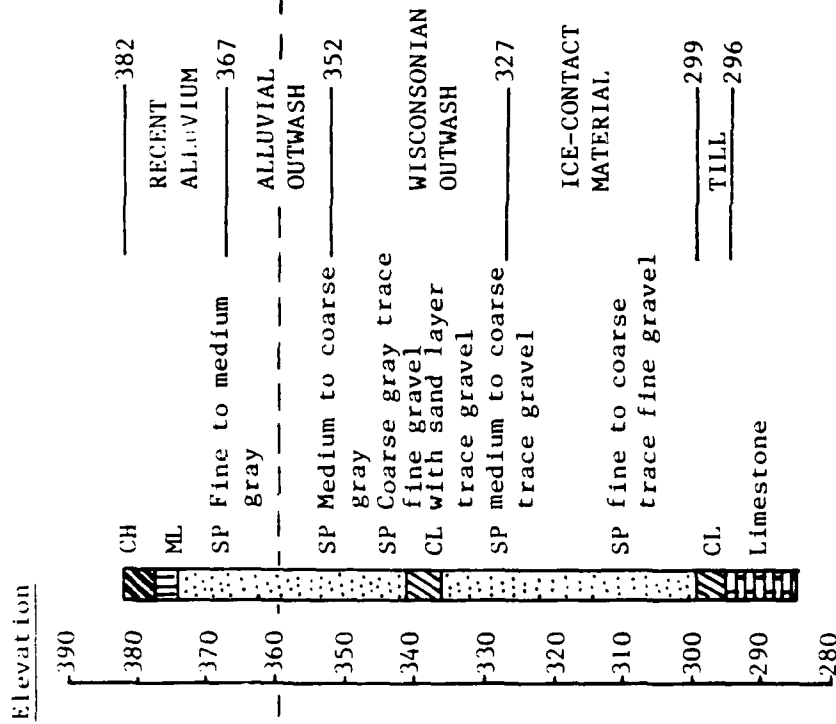


FIG. 2. Location of Pile Groups Within Phase 1 of Construction

Pile Group 1



Pile Group 2

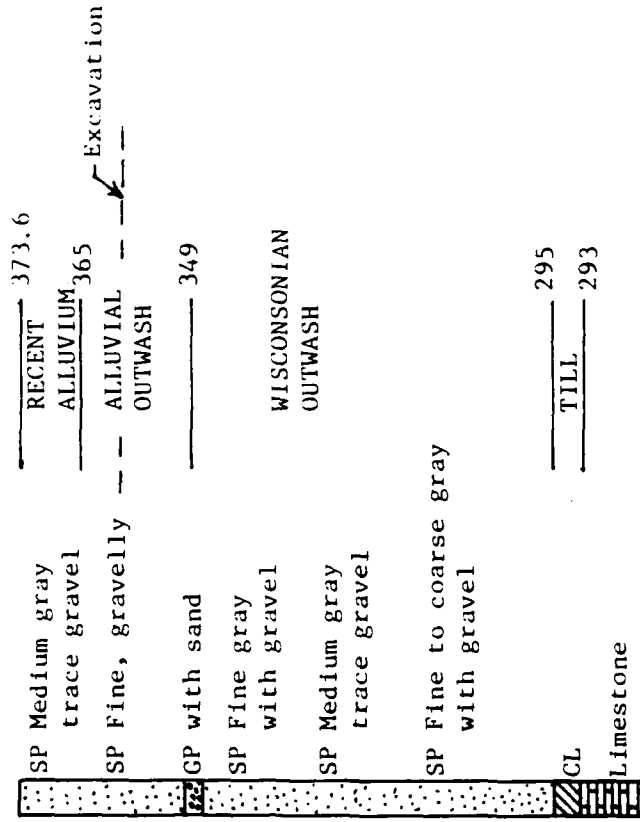


FIG. 3. Soil Profile Across Test Site



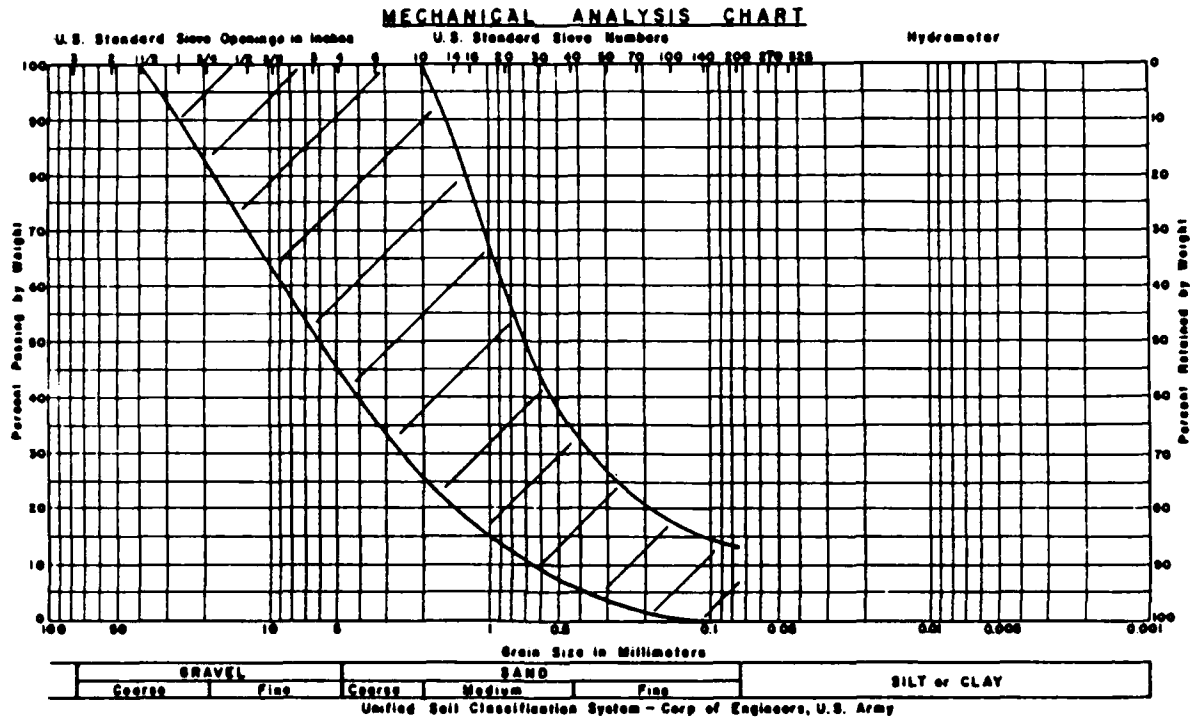


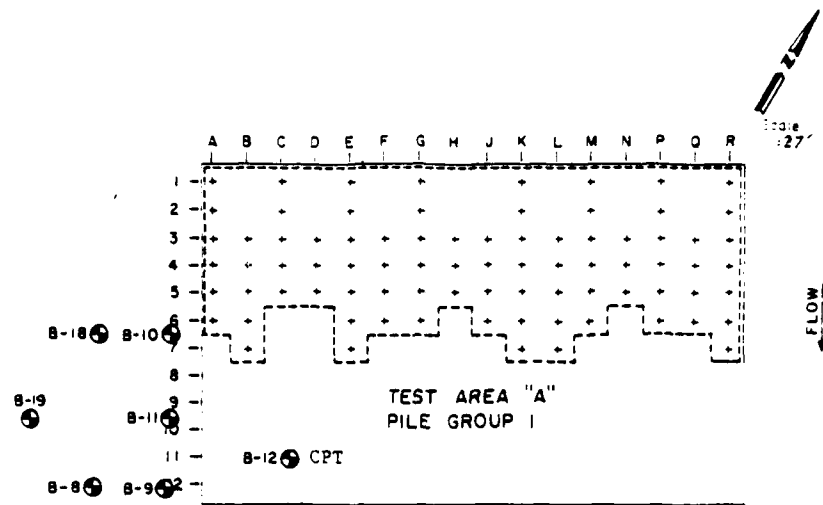
FIG. 4. Gradation Band of Sieve Analysis Test Samples Obtained from SPT

The in situ test investigation consisted of 4 cone penetration test (CPT) soundings, 4 SPT borings and 12 pressuremeter test (PMT) borings. The location of the borings is shown on Figures 5 to 7 for the three pile groups.

The CPT soundings were performed with a 20-ton cone truck pushing an electrical cone with point, friction sleeve and pore pressure measurements. The CPT results are presented in Figure 8.

The SPT borings were performed with both the standard split spoon sampler according to ASTM D 1586 and also with a 3-in. outside diameter split spoon sampler driven by a 350-lb hammer with an 18 in. drop. A correlation between these two test procedures showed (Briaud et al. 1984) that the SPT blow count is approximately equal to 1.5 times the blow count from the 3-in. sampler. This correlation has been used when necessary to obtain SPT profiles for the three pile groups. The SPT results are shown in Figure 9.

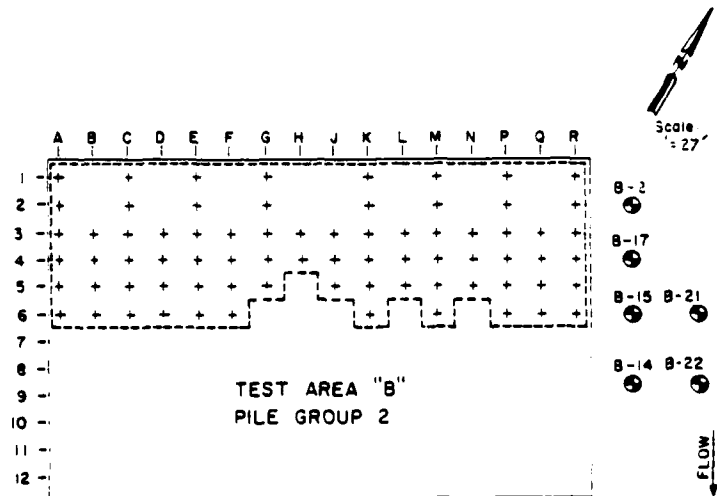
Six different pressuremeters were used in the site investigation. They were the Menard, Oyo, Pavement, Slotted Tube, WES and TEXAM pressuremeters. All pressuremeters except the Slotted Tube and Pavement pressuremeters were inserted into a predrilled borehole prepared by rotary drilling with axial injection of drilling mud. The Slotted Tube pressuremeter was driven into the soil with the SPT hammer and the Pavement pressuremeter was inserted into a hand-augered borehole. The pressuremeter tests resulted in profiles of net limit pressure ( $p_L^*$ ), initial modulus ( $E_0$ ) and reload modulus ( $E_r$ ) which are shown in Figures 10, 11 and 12 for pile groups 1, 2 and 3 respectively. The results from the six pressuremeters compare quite well; most of the variation in results



Note:  
Piles inside dashed area  
were present when borings  
were made.

B-3 SPT

FIG. 5. In Situ Tests Borings for Pile Group 1



Note:  
Piles inside dashed area  
were present when borings  
were tested.

FIG. 6. In Situ Tests Borings for Pile Group 2

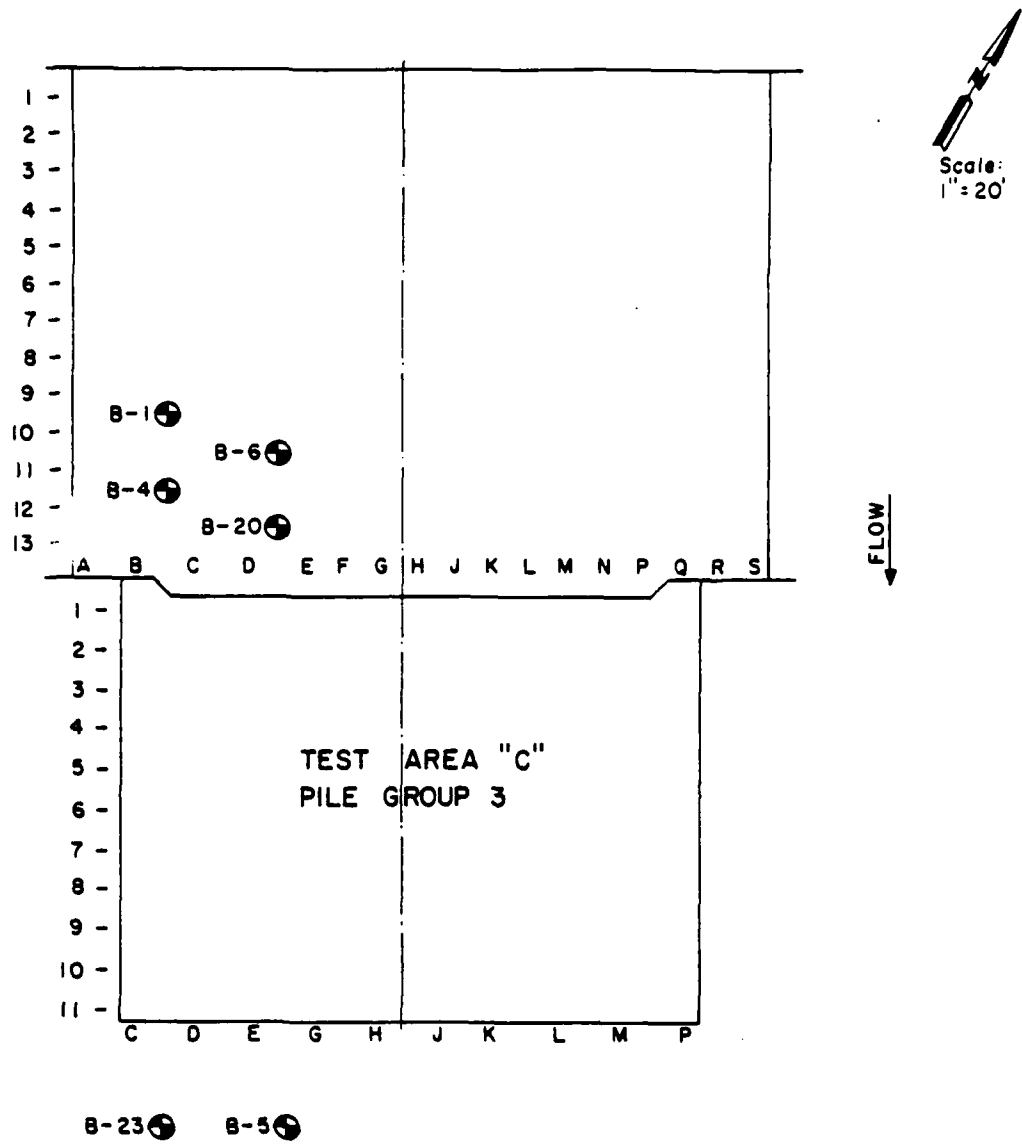


FIG. 7. In Situ Tests Borings for Pile Group 3

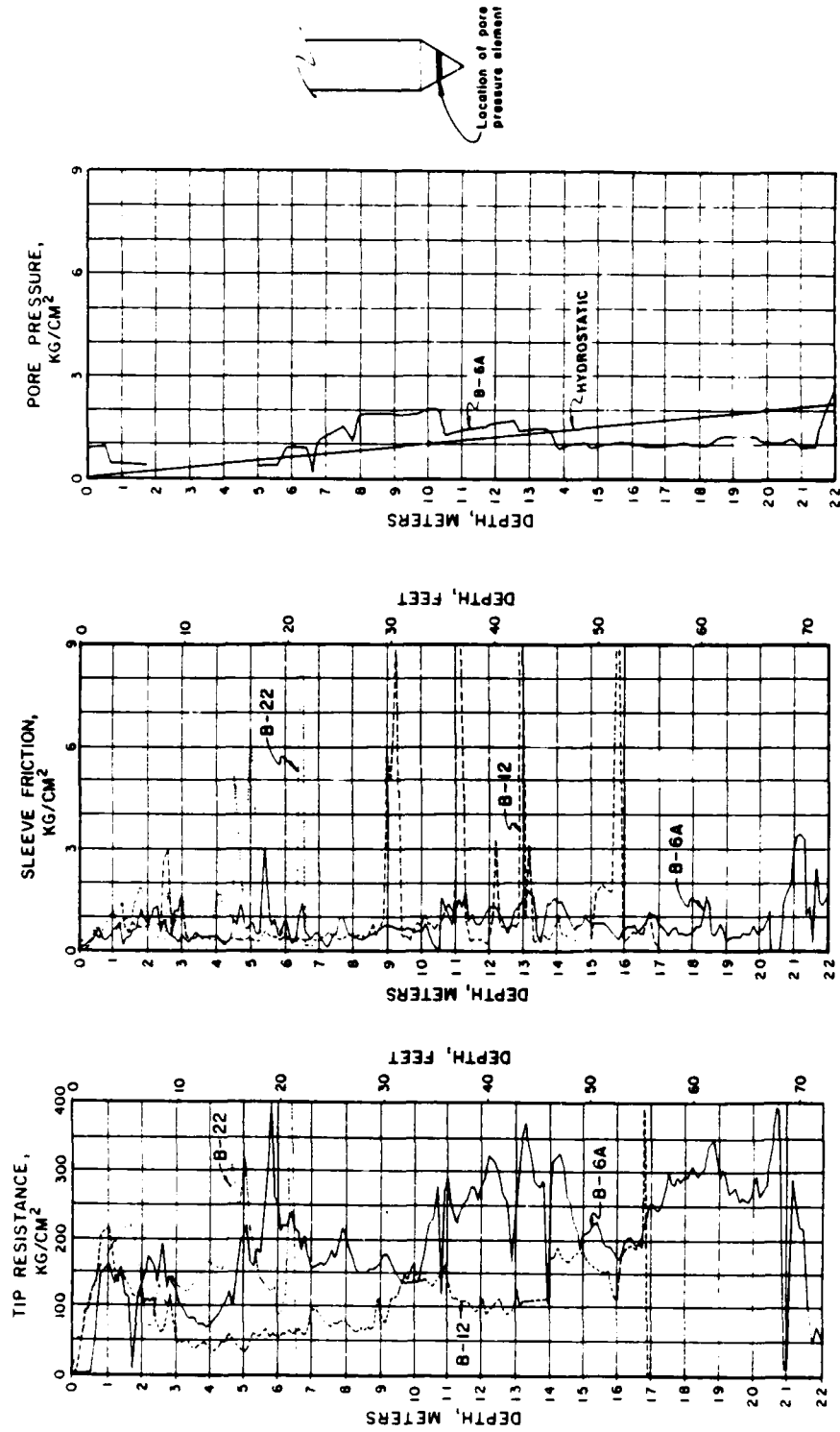
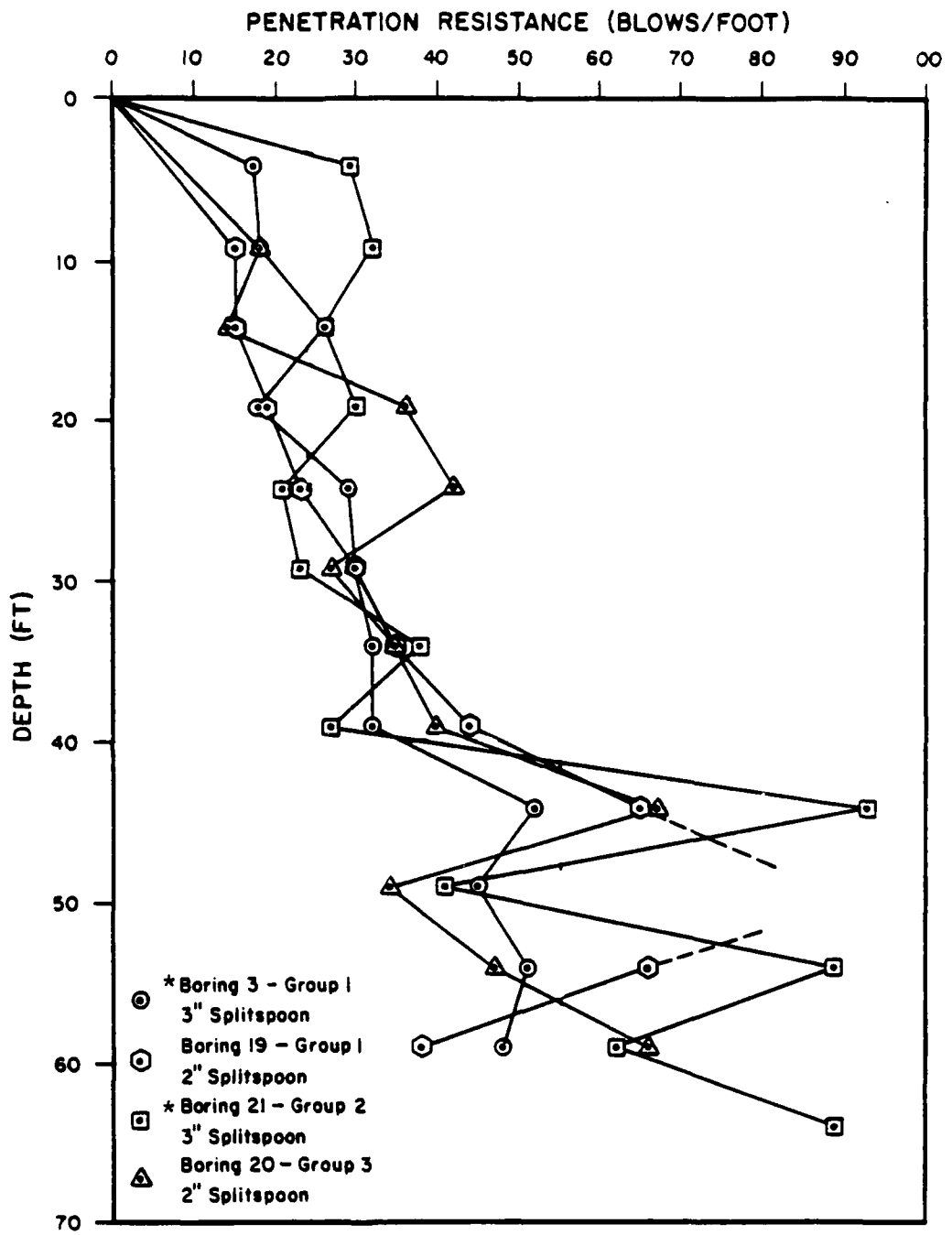


FIG. 8. Cone Penetration Test Soundings



\* NOTE: Penetration Resistance Shown has been multiplied by 1.5

FIG. 9. Standard Penetration Test Profiles

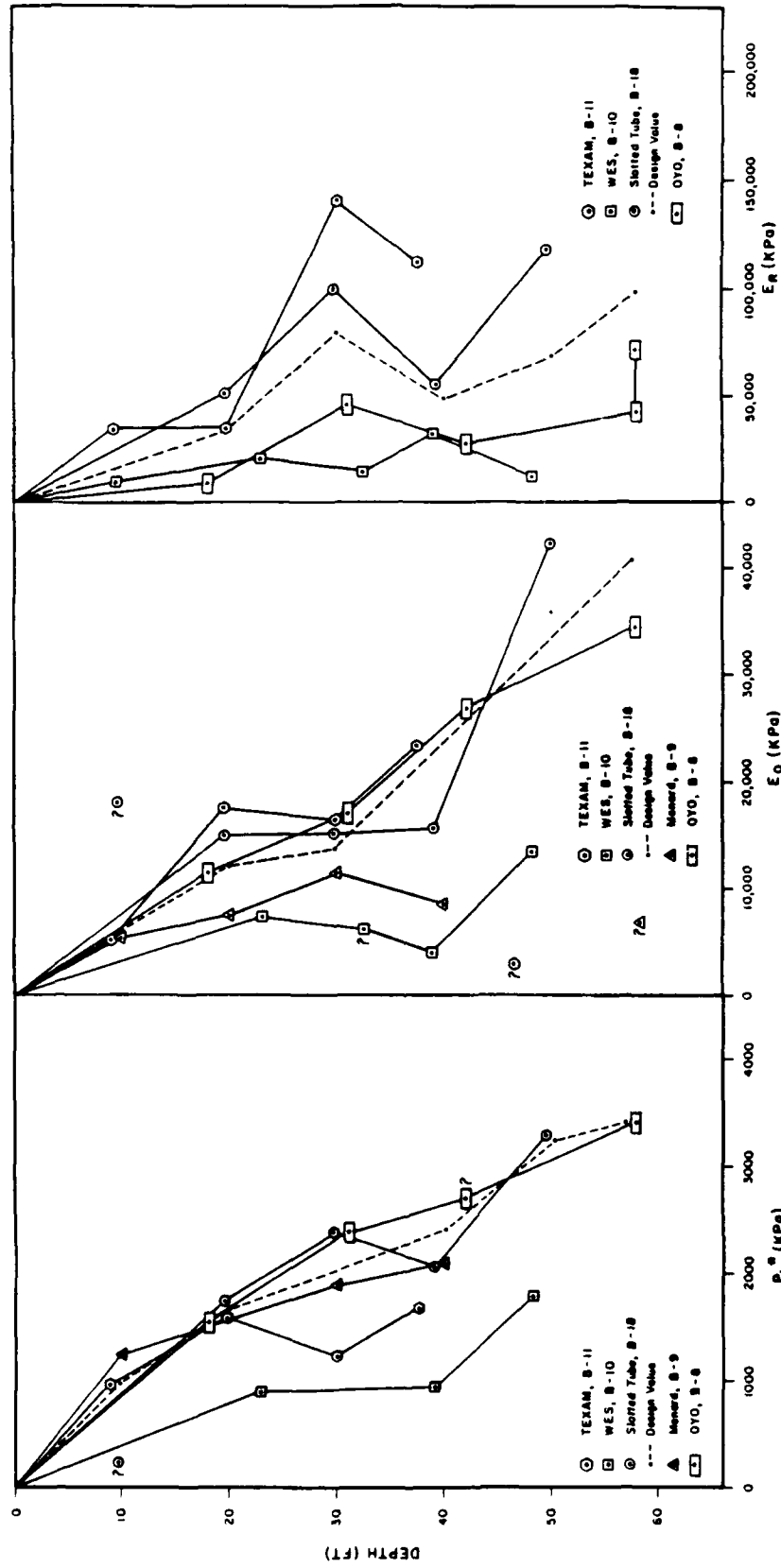


FIG. 10. Pressuremeter Parameter Profiles for Pile Group 1

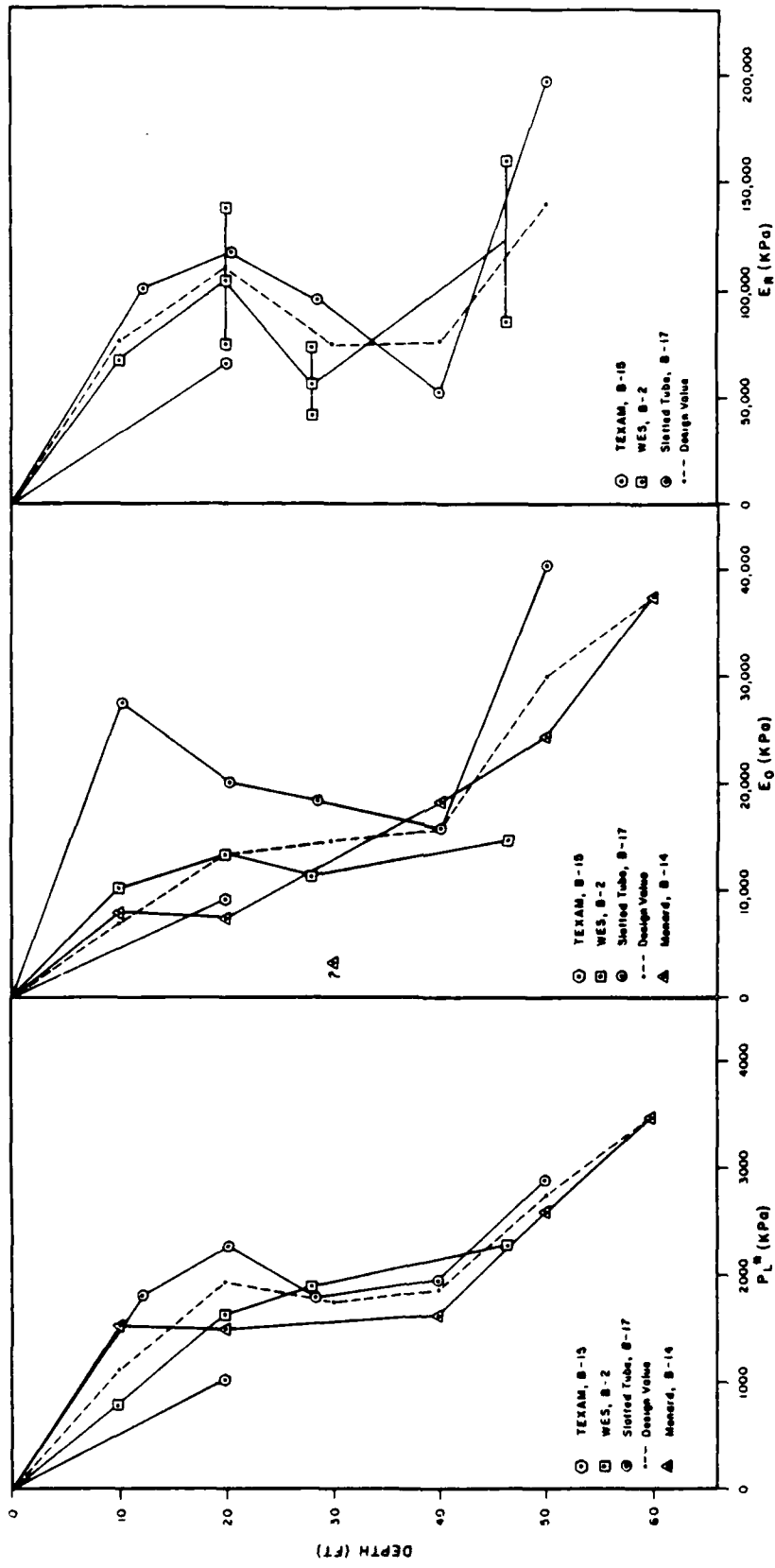


FIG. 11. Pressuremeter Parameter Profiles for Pile Group 2



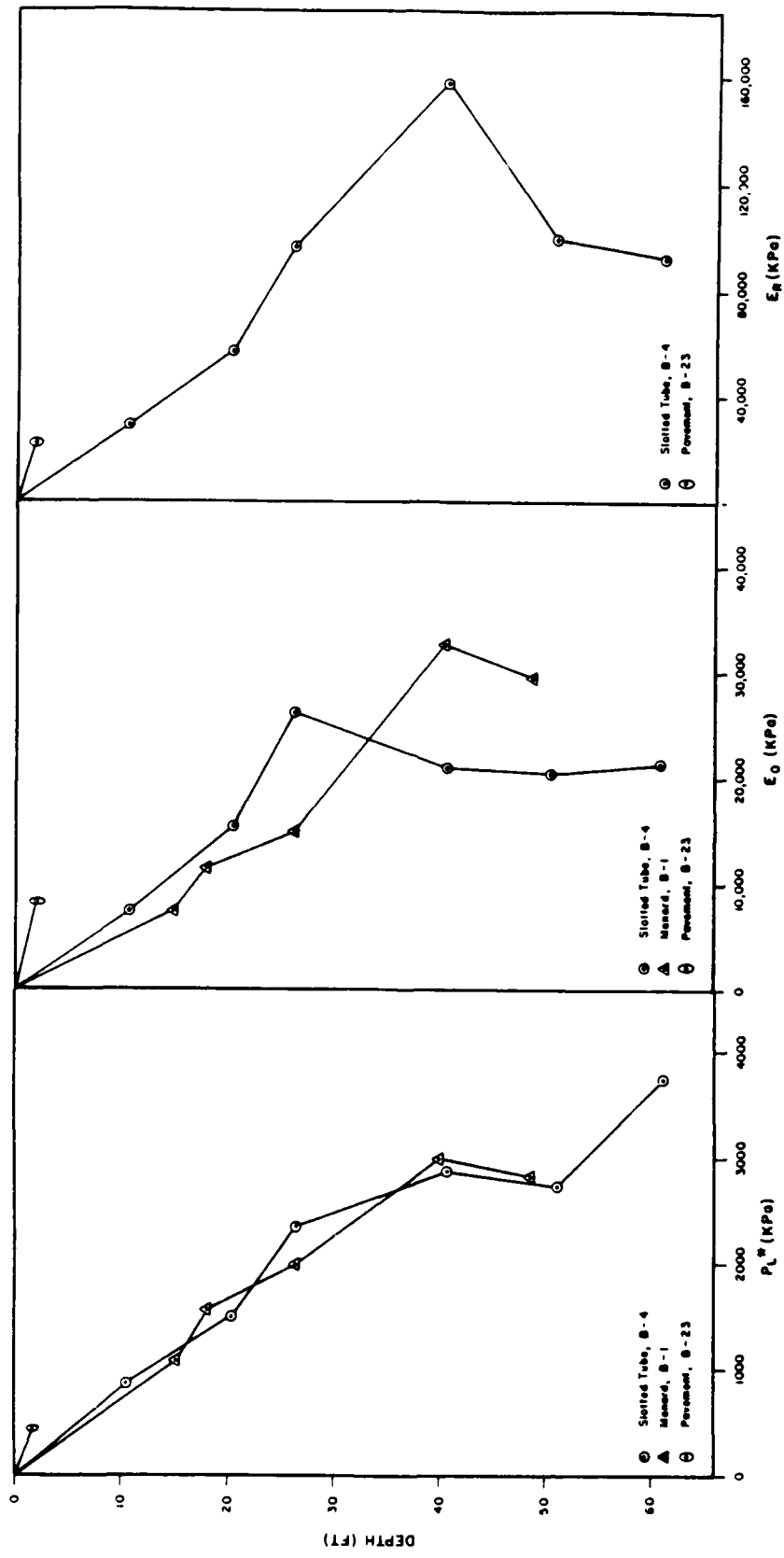


FIG. 12. Pressuremeter Parameter Profiles for Pile Group 3

can probably be attributed to actual variation in the soil rather than differences between pressuremeters. The values of the pressuremeter parameters used in the predictions are shown in the figures for each pile group.

### 2.3 Soil Variability

A series of approximately 400 over-water borings was performed across the entire dam site before construction. An area 400 ft by 200 ft corresponding to the pile test location was selected (Briaud and Tucker 1984) which contained 13 SPT borings. In order to obtain an indication of the soil variability, the soil was divided into 5 ft thick horizontal layers. All the SPT blowcounts within one layer from the 13 borings were analyzed to obtain the mean, standard deviation and coefficient of variation. This process was performed for each layer. The results are shown in Table 1. This analysis indicates that the average

Table 1. Horizontal Variability of SPT Data

Depth (ft)	Mean (blows/ft)	Standard Deviation (blows/ft)	Coefficient of Variation
0-15	57.3	35.8	0.624
15-20	14.7	5.2	0.356
20-25	13.8	4.6	0.335
25-30	17.3	3.2	0.185
30-35	19.5	6.2	0.317
35-40	21.2	6.0	0.274
40-45	26.6	7.7	0.291
45-50	28.9	6.9	0.238
50-55	33.6	14.8	0.440
55-60	27.3	10.2	0.373
60-65	36.2	16.1	0.445
65-70	44.8	20.9	0.467
70-75	48.1	18.7	0.389
75-80	63.2	22.4	0.355
80-90	74.1	40.9	0.552
Average	35.1	14.6	0.376

horizontal coefficient of variation is 37.6%. It is reasonable to expect that the pile capacities across the site vary by at least that amount.

### 3. THE AXIAL PILE LOAD TEST PROGRAM

#### 3.1 Objectives

The axial pile load test program was undertaken to investigate the effect of several factors on the compression and tension capacities of driven steel H and pipe piles (Conroy 1985). The main objectives of the program were to study

- . the effect of load test procedure on pile capacity (ASTM Standard vs. ASTM Quick)
- . the effect of pile batter on pile capacity
- . H pile vs. pipe pile capacity
- . pile capacity variation across the site

#### 3.2 The Piles

The load test program consisted of 13 tension and 9 compression tests on driven HP14x73 piles and one tension and one compression test on 12 in., 14 in. and 16 in. diameter pipe piles. The H-piles varied in length from 37 ft to 71 ft. The pipe piles varied in length from 36 ft to 48 ft. The pipe piles were filled with sand during the tension tests and with concrete during the compression tests. The piles were driven on a 5 ft center-to-center spacing (Figures 5 to 7). The time between driving and the start of the load test ranged from 4 to 133 days and averaged 22 days (Table 2). The were loaded to a maximum of 400 tons in compression and 150 tons in tension or until the pile continued to move with no further increase in load. Details of the piles are given in Table 2.

Sixteen of the H-piles were instrumented with six levels of tell tales to obtain profiles of deflection versus depth during the load tests. The tell tales were mounted, after driving, within two channels

Table 2. Description of Piles

File	Date Driven	Begin Load Test	Test Type	Pile Type	Axial		Blowcount at Final Penetration (blows/ft)
					Pile Length (ft)	Batter	
1-1	8/14/82	8/18/82	Standard Tension	HP14x73	60.75	Vert	65
1-2	8/25/82	8/29/82	Standard Tension	HP14x73	54.00	Vert	29
1-3A	8/26/82	9/02/82	Standard Comp.	HP14x73	54.00	Vert	31
1-3B	8/26/82	9/05/82	Standard Tension	HP14x73	54.00	Vert	31
1-4	9/10/82	9/14/82	Standard Tension	HP14x73	65.00	1:2.5	81
1-5	9/10/82	9/18/82	Quick Tension	HP14x73	60.50	Vert	63
1-6	10/07/82	10/18/82	Quick Comp.	HP14x73	53.00	Vert	38
1-7	9/24/82	10/04/82	Quick Comp.	HP14x73	59.00	Vert	79
1-8	9/22/82	9/27/82	Quick Comp.	HP14x73	66.00	1:2.5	70
1-9	9/23/82	9/30/82	Quick Comp.	HP14x73	58.00	1:2.5	29
2-1	8/25/82	8/30/82	Quick Tension	HP14x73	55.00	Vert	21
2-2	8/18/82	8/24/82	Quick Tension	HP14x73	59.00	1:2.5	32
2-3	8/27/82	9/03/82	Quick Tension	HP14x73	69.20	1:2.5	75
2-4	8/26/82	8/31/82	Standard Tension	HP14x73	58.00	1:2.5	20
2-5	9/28/82	10/06/82	Standard Comp.	HP14x73	59.00	1:2.5	24
2-6	9/13/82	9/23/82	Standard Comp.	HP14x73	71.17	1:2.5	73
2-7	9/16/82	9/29/82	Standard Comp.	HP14x73	66.83	Vert	79
2-8	10/29/82	11/03/82	Standard Tension	HP14x73	40.00	Vert	NA
3-1	12/01/82	12/28/82	Standard Comp.	12" Pipe	46.70	Vert	13
3-2	12/01/82	1/04/83	Standard Tension	12" Pipe	36.00	Vert	40
3-4	12/01/82	1/03/83	Standard Comp.	14" Pipe	47.20	Vert	28
3-5	12/01/82	12/28/82	Standard Tension	14" Pipe	36.50	Vert	17
3-7	12/01/82	1/07/83	Standard Comp.	16" Pipe	47.80	Vert	22
3-8	12/01/82	12/29/82	Standard Tension	16" Pipe	36.50	Vert	32
3-10	12/28/82	1/06/83	Standard Comp.	HP14x73	65.67	Vert	80
3-14	11/18/82	3/14/83	Quick Tension	HP14x73	39.00	Vert	21
3-15	11/10/82	3/23/83	Quick Tension	HP14x73	37.00	Vert	3
3-16	3/25/83	4/27/83	Quick Tension	HP14x73	37.00	Vert	17

(C4x7.25) welded to each side of the web of the H-piles. The deflections were monitored using manually-read dial gauges mounted on the piles at the top of the tell tales. For the remainder of the piles, only the top load and settlement were obtained.

The piles were driven with an ICE 640 diesel pile driving hammer with a rated maximum energy of 40,000 ft-lbs. The average blow count for the last foot of penetration ranged from 9 to 38 blows per foot

(bpf) with an average of 25 bpf for the short piles which stopped in the soil above the bedrock, and from 63 to 81 bpf with an average of 74 bpf for the long piles driven to bedrock. The blow counts for each pile are given in Table 2 and typical logs of blow count versus depth for a short pile and a long pile are shown in Figures 13 and 14 respectively.

### 3.3 The Load Test Procedures

The load tests were carried out according to the ASTM D1143-74 Standard and Quick procedures. Minor changes were made in the ASTM procedures because increased accuracy in the measurement systems and additional displacement readings were required. Also, the unloading portion of the tests was shortened in order to reduce the time necessary to run the tests. Table 2 indicates which piles were tested using the Standard procedure and which piles were tested using the Quick procedure.

### 3.4 Definition of Measured Ultimate Load

In order to compare the measured results with predictions, or to use the load tests results in a design, a criterion must be specified to determine the ultimate load. This is especially necessary for pile load tests in sand where a plunging load is seldom obtained. In this study the ultimate load was defined as the load,  $P_{ult}$ , corresponding to a settlement,  $s$ :

$$s = \frac{D}{10} + \frac{P_{ult}L}{AE}$$

- D - equivalent pile diameter
- L - pile length
- A - pile cross-sectional area
- E - pile modulus of elasticity

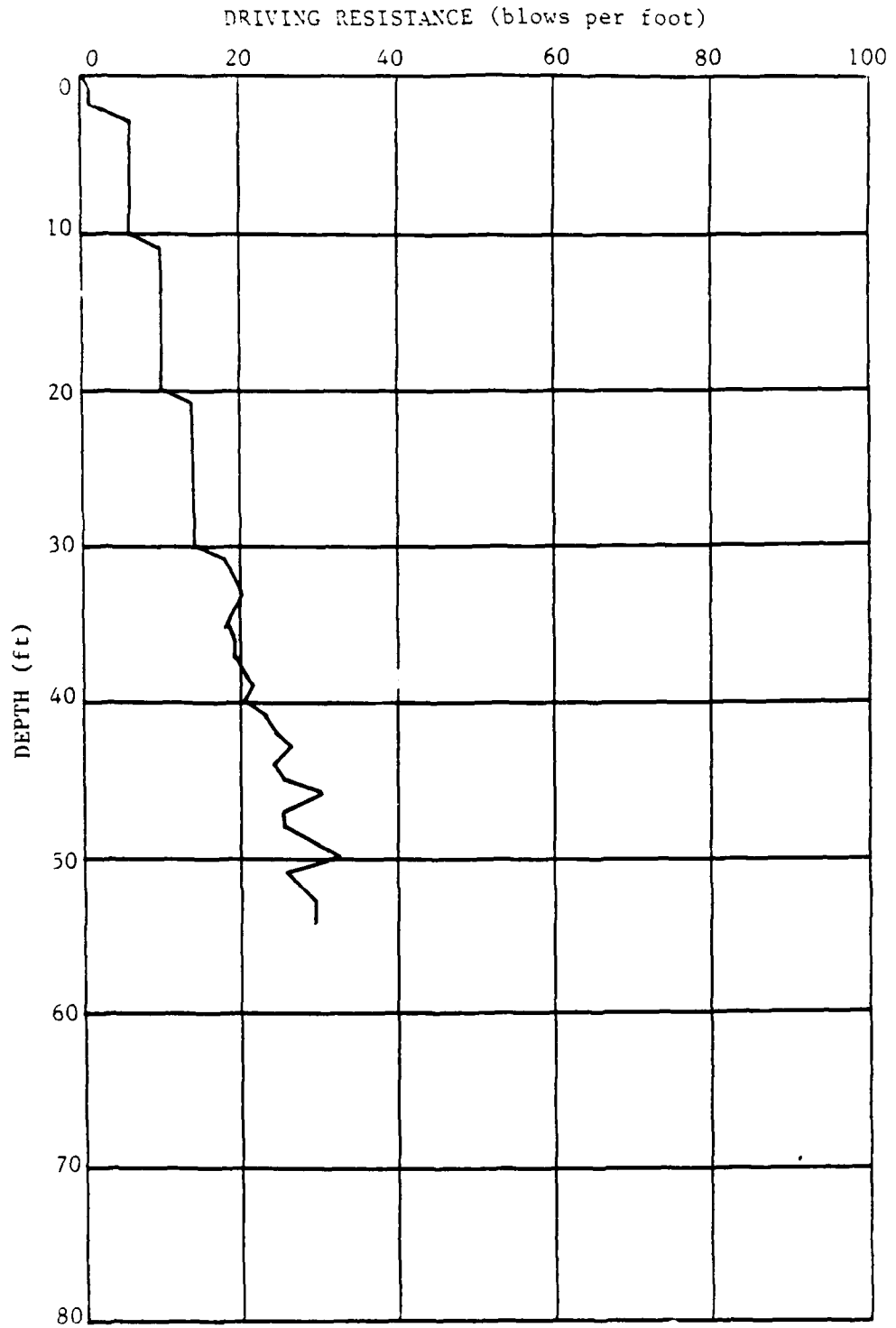


FIG. 13. Typical Driving Resistance Profile for Pile Terminating Above Rock

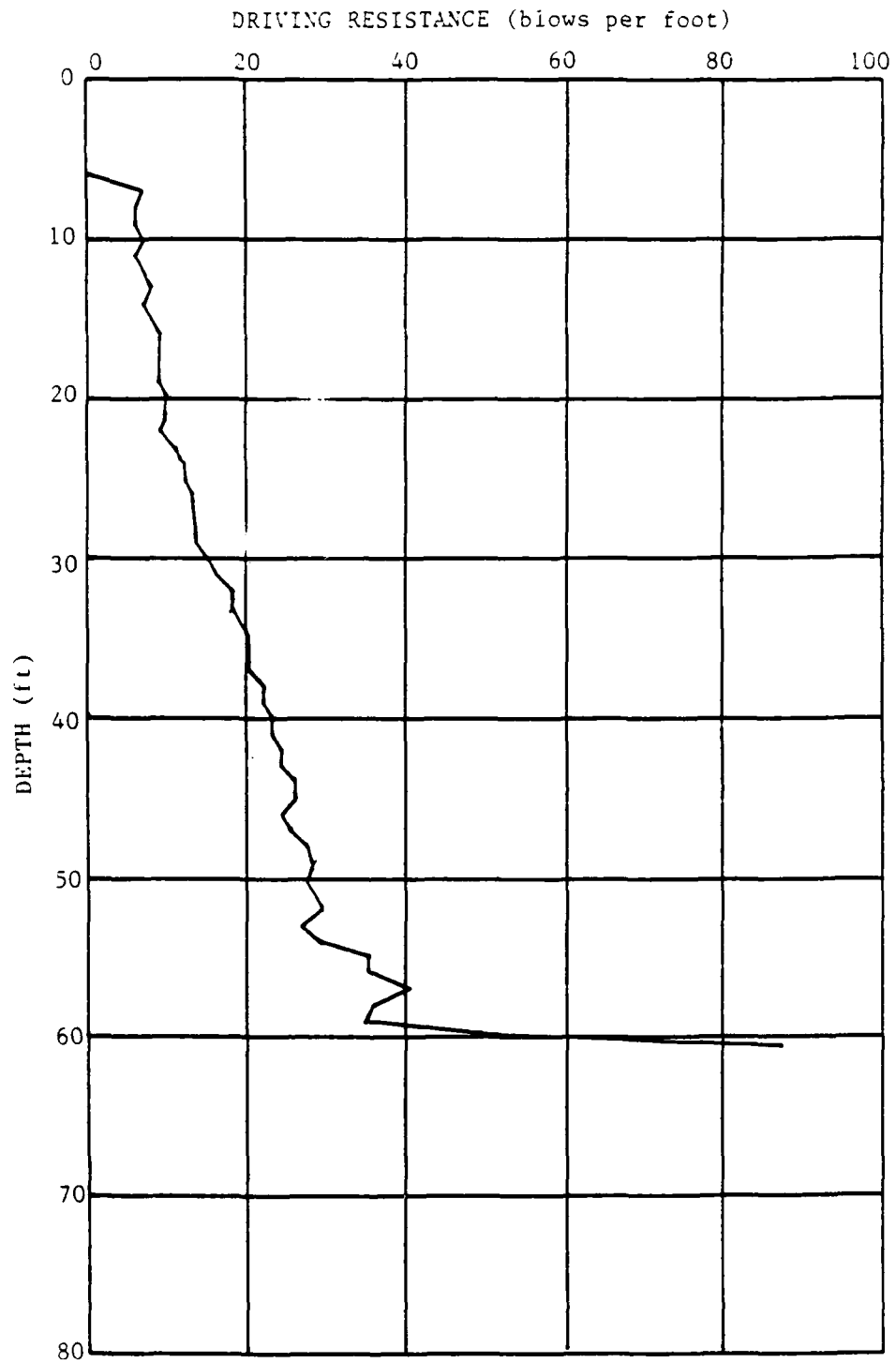


FIG. 14. Typical Driving Resistance Profile for Pile Driven to Rock



### 3.5 Load Test Results

The load tests have been divided into six groups based on pile type, depth of penetration and test type. The six groups are as follows:

1. H-piles - driven to rock - compression tests
2. H-piles - driven to rock - tension tests
3. H-piles - stopped above rock - compression tests
4. H-piles - stopped above rock - tension tests
5. Pipe piles - stopped above rock - compression tests
6. Pipe piles - stopped above rock - tension tests

3.5.1 Ultimate Loads. The load-settlement curves for the categories above are shown in Figures 15 to 20 with individual piles marked. Also marked on these figures are the orientation of the pile and the test procedure used. The ultimate loads according to the definition in Section 3.4 are shown in Table 3 with their corresponding settlements. The load tests on the H-piles which were driven to rock did not achieve enough movement in either compression or tension to determine an ultimate load. Also shown in Table 3 are the allowable loads for a factor of safety of 2 with their corresponding settlements and stiffness values. The stiffness is defined as the allowable load divided by the corresponding settlement. Since the load-settlement curves are approximately linear up to this point the stiffness is simply the initial slope of the load-settlement curve.

Since the H-piles were instrumented, the load distribution between side load and point load could be determined. The distribution is shown in Table 4 for the four short H-piles tested in compression. Except for

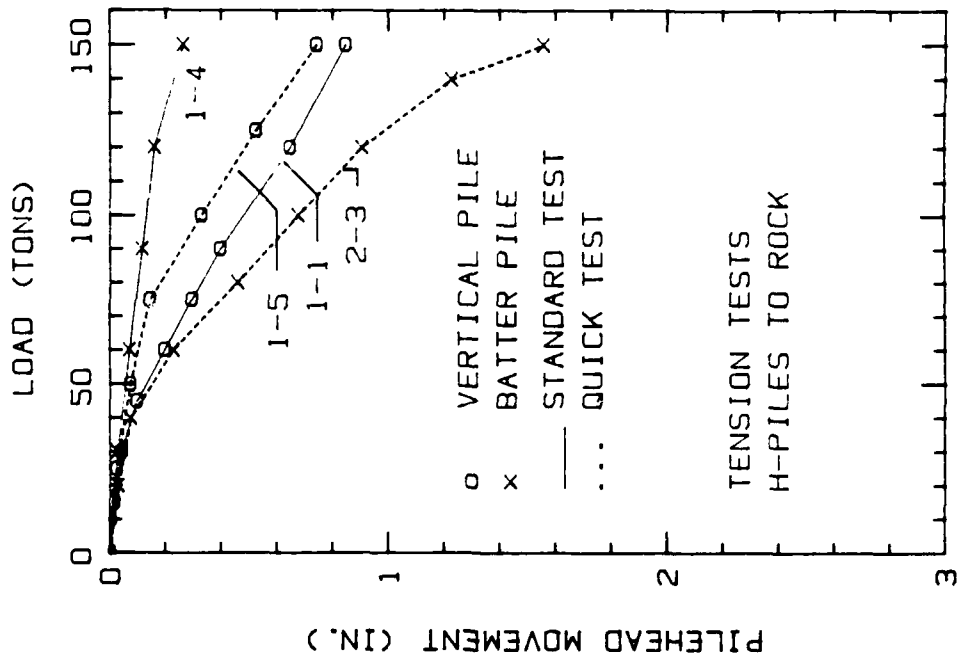


FIG. 16. Load Test Results for Tension Tests on H-Piles Driven to Rock

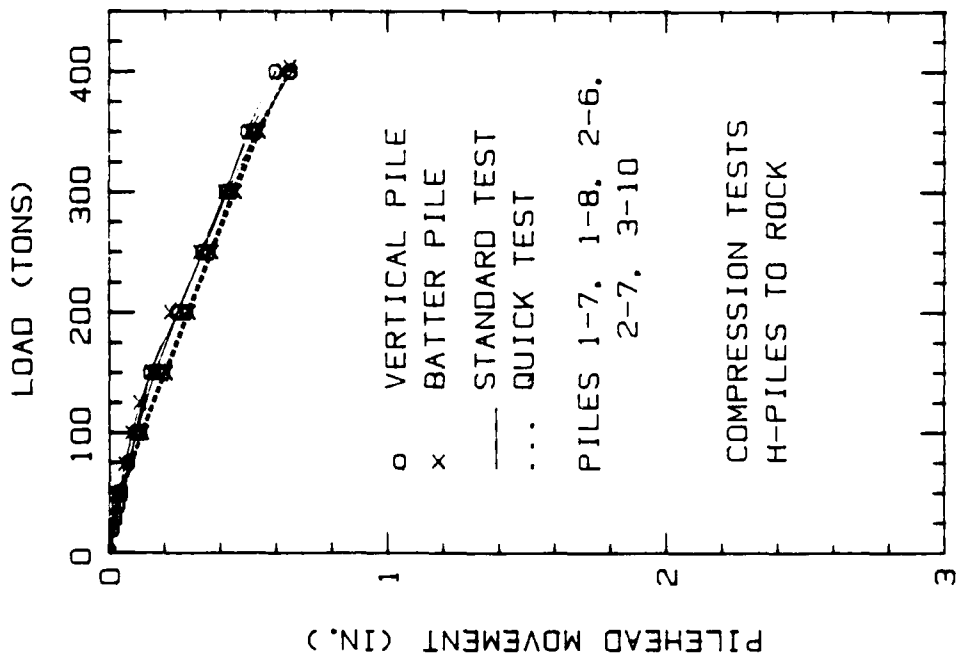


FIG. 15. Load Test Results for Compression Tests on H-Piles Driven to Rock

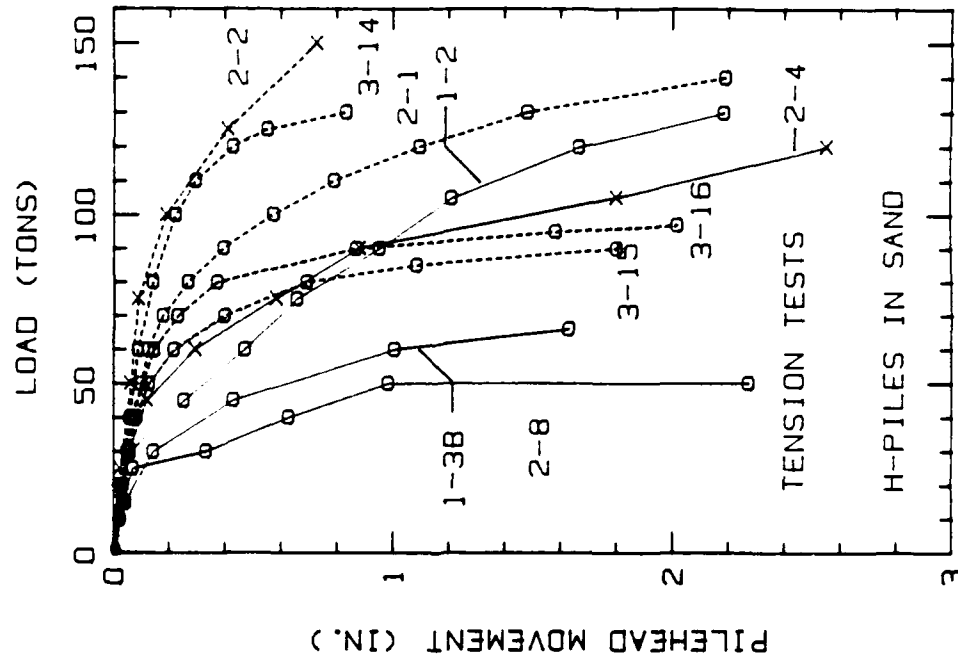


FIG. 18. Load Test Results for Tension Tests on H-Piles in Sand

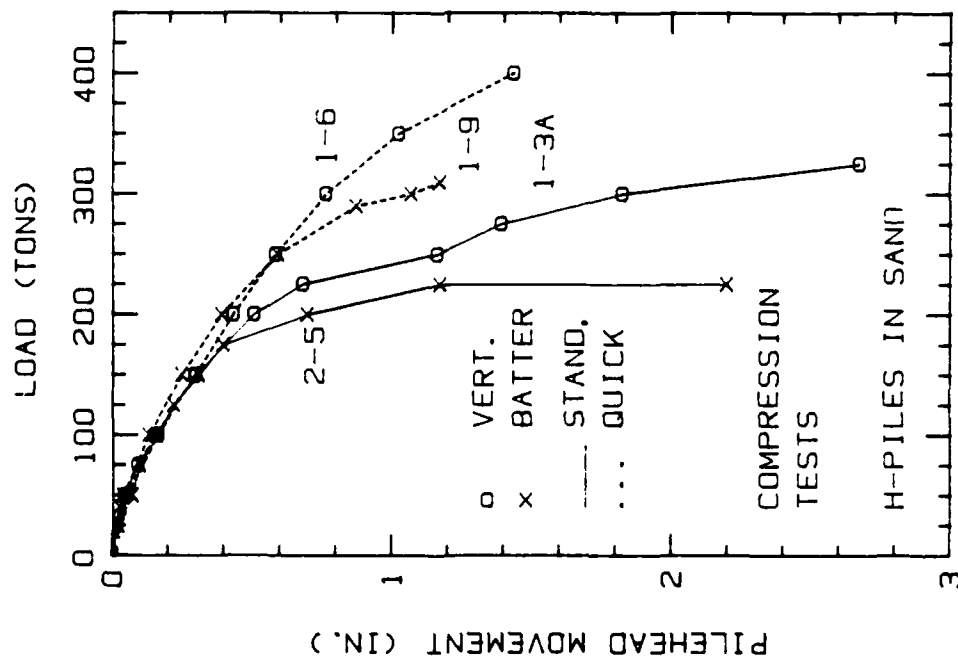


FIG. 17. Load Test Results for Compression Tests on H-Piles in Sand

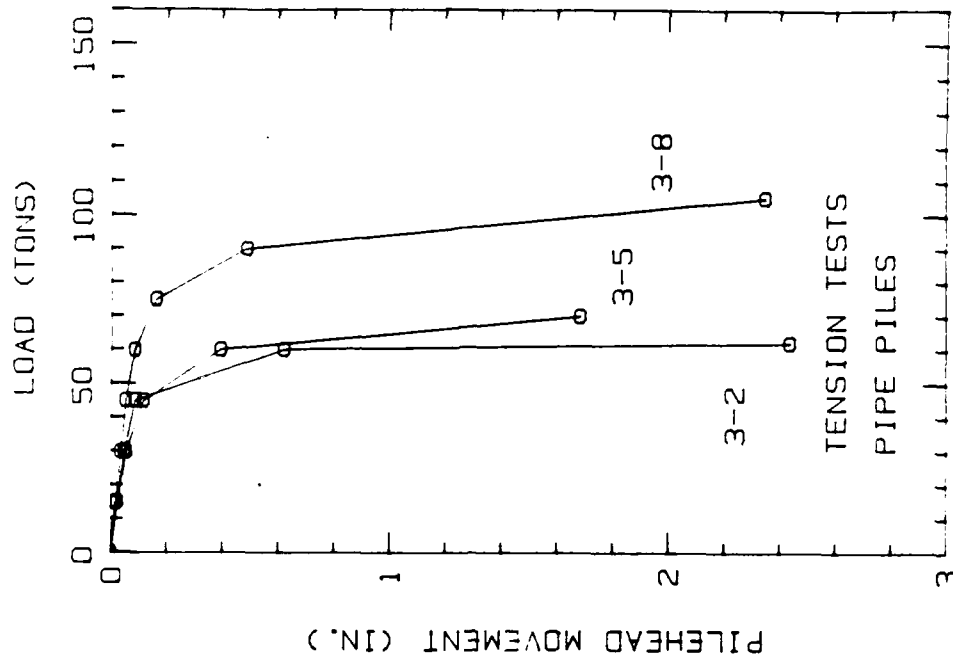


FIG. 20 Load Test Results for Tension Tests on Pipe Piles

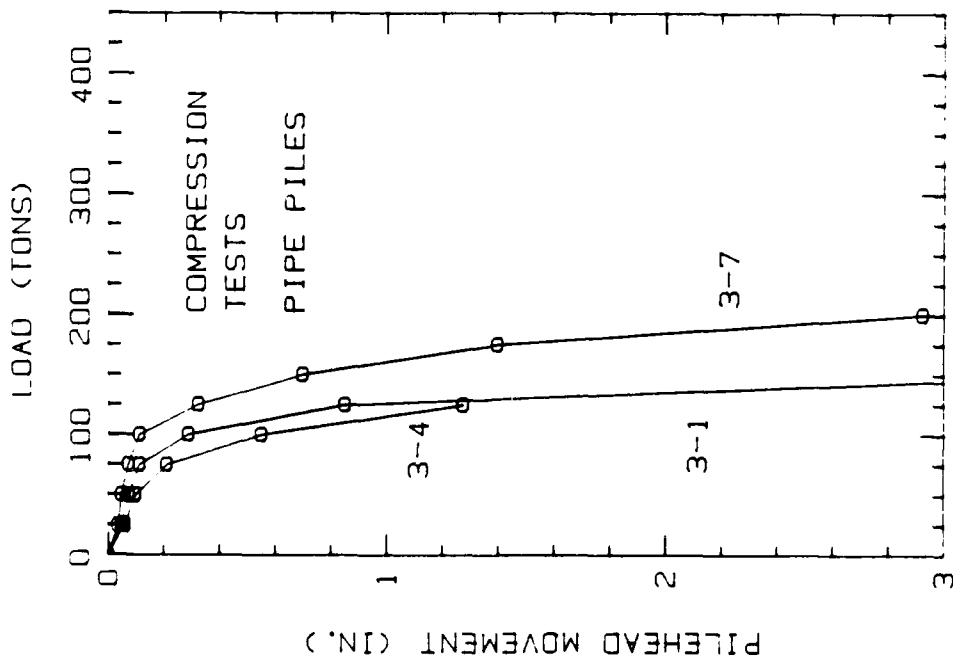


FIG. 19. Load Test Results for Compression Tests on Pipe Piles

Table 3. Pile Load Test Results

Pile	Ultimate Load (tons)	Settlement (in.)	Allowable Load (tons)	Settlement (in.)	Stiffness (tons/in)
1-1	*				
1-2	122.5	1.80	61.3	0.49	125
1-3A	313.0	2.12	156.5	0.33	477
1-3B	66.7	1.70	33.3	0.21	160
1-4	*				
1-5	*				
1-6	428.0	2.30	214.0	0.48	448
1-7	*				
1-8	*				
1-9	337.0	2.20	168.5	0.31	553
2-1	136.0	1.82	68.0	0.17	403
2-2	*				
2-3	156.0	1.93	78.0	0.44	178
2-4	106.0	1.78	53.0	0.21	249
2-5	225.0	2.00	112.5	0.19	580
2-6	*				
2-7	*				
2-8	50	1.65	25.0	0.07	357
3-1	132.1	1.62	66.1	0.10	664
3-2	60.8	1.35	30.4	0.05	584
3-4	130.0	1.63	65.0	0.17	387
3-5	68.5	1.49	34.3	0.08	456
3-7	183.0	1.89	91.5	0.10	914
3-8	99.9	1.72	50.0	0.07	739
3-10	*				
3-14	*				
3-15	90.0	1.69	45.0	0.11	426
3-16	96.0	1.70	48.0	0.10	494

\* Pile did not reach failure.

Table 4. Load Distribution in Compression Tests

Pile	Side Load (tons)	Point Load (tons)	Total Load (tons)
1-3A	161	152	313
1-6	353	75	428
1-9	252	85	337
2-5	179	46	225

pile 1-3A, the piles carried from 75% to 82% of the load in friction.

The average ultimate unit side friction for the H-piles tested in tension was 0.62 ksf (using the outside perimeter), while the average of the pipe piles was 0.77 ksf, or approximately 24% higher than the H-piles. This could be due to the larger volume of soil displaced by the pipe piles which were driven closed ended.

**3.5.2 Residual Loads.** During each hammer blow, the pile moves downward, rebounds and then oscillates around a final position. At its final position the pile is in equilibrium under a certain point load and a certain friction load. These two loads are equal and opposite since the load at the pile head is zero. In a conventional load test these residual loads are ignored because the instrumentation is zeroed after driving the pile, thus assuming that the pile is stress-free after installation. If a tension test is performed on such a pile, the instrumentation will register a tension load at the pile tip which increases during the load test. If the pile is pulled far enough, this point load will increase to the value of the residual point load after driving and then remain constant throughout the rest of the test. The residual loads could be obtained in this manner for four piles in this load test program. As can be seen in Table 5, the residual load was as high as 52 tons and averaged 26.5 tons, which is 30% of the average ultimate point load measured in the compression tests. This illustrates the fact that the residual loads can greatly affect the interpretation of load test results when load distribution data is needed. The residual loads were not measured for any of the compression tests in this load test program.

Table 5. Measured Residual Point Loads

File	Residual Point Load (tons)	Ultimate Load (tons)
1-2	20	122.5
1-3B	34	66.7
2-1	52	136
2-3	0	156

3.5.3 Shape of Load-Settlement Curve. The load-settlement curves have been replotted after normalization to the defined point of failure. The normalized load is the load divided by the failure load and the normalized settlement is the settlement divided by the settlement at the failure load. The resulting plots are shown in Figures 21 to 24. These plots reveal that the shape of the load-settlement curves are very similar, especially for the pipe piles. It also shows that at working loads (normalized load = 0.5) the relative movements for the compression tests are larger than for the tension tests, being 81% larger for the H-piles and 67% larger for the pipe piles. These figures also show that the H-piles have a relative movement at working loads which is approximately twice that of the pipe piles in both tension and compression. This may again be due to the fact that the H-piles are low displacement piles whereas the pipe piles which were driven closed-ended were full displacement piles.

3.5.4 Effect of Pile Batter. In order to quantify the effect of pile batter on the pile response, the allowable loads and stiffnesses of similar piles are compared in Table 6. The piles were compared if the lengths were similar and if the test procedure was the same. In tension, the allowable load for the battered pile was 12.1% higher than that of the vertical piles. In compression, however, the allowable load

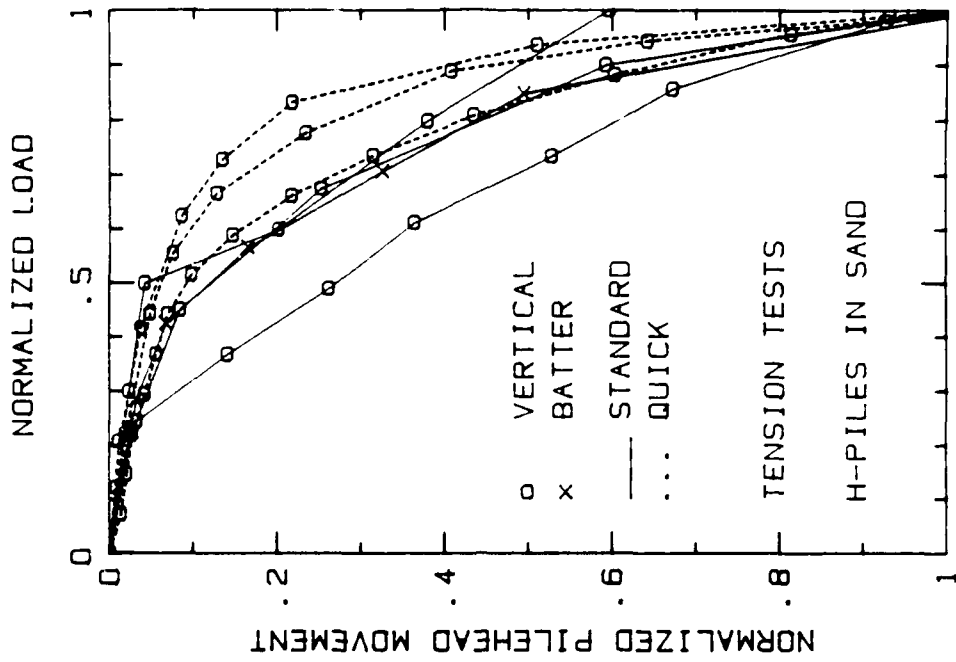


FIG. 22. Normalized Load-Settlement Curves for Tension Tests on H-Piles

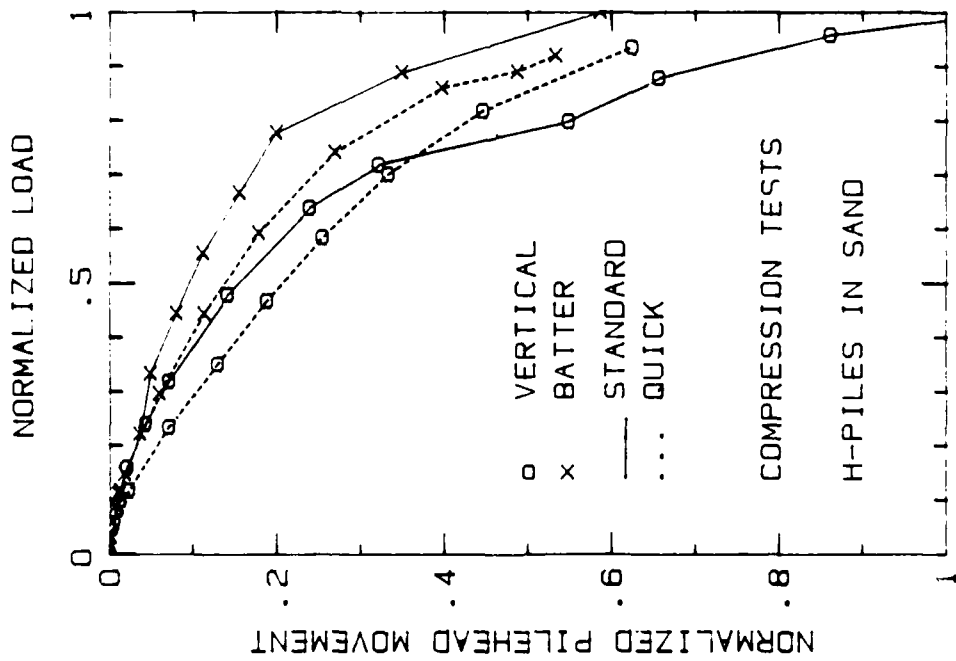


FIG. 21. Normalized Load-Settlement Curves for Compression Tests on H-Piles



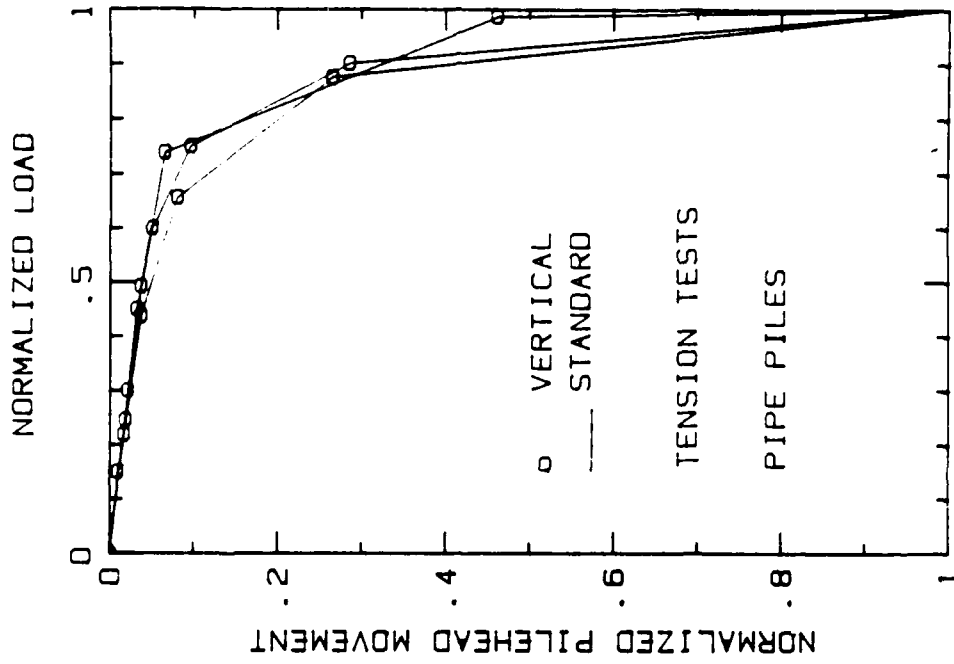


FIG. 24. Normalized Load-Settlement Curves for Tension Tests on Pipe Piles

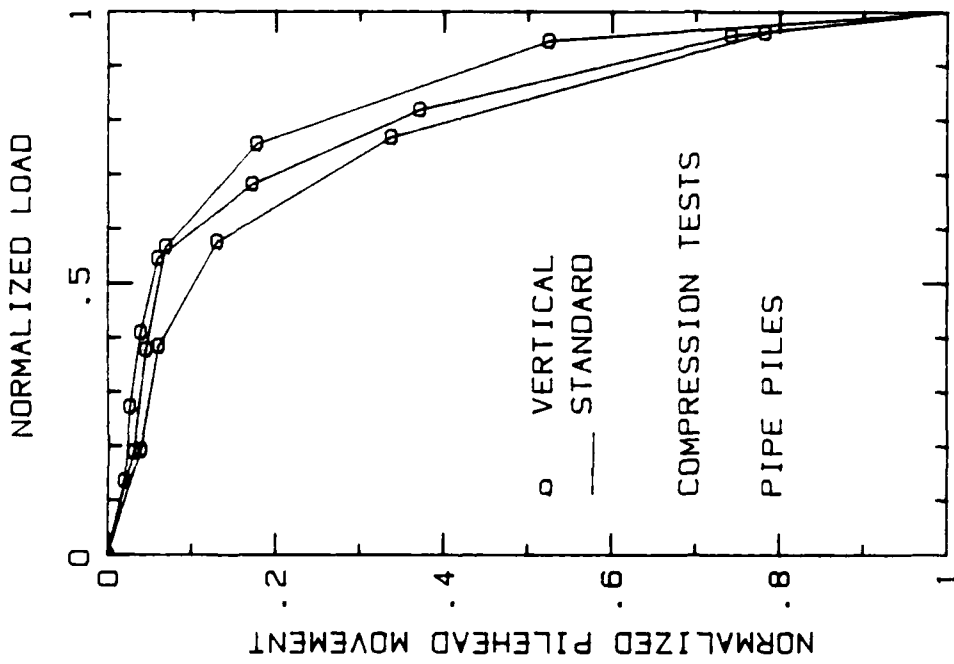


FIG. 23. Normalized Load-Settlement Curves for Compression Tests on Pipe Piles

Table 6. Comparison of Vertical and Battered Pile Response

Pile	Vertical	Battered	Battered/Vertical (%)
Allowable Load (tons)			
<b>Tension</b>			
1-2	61.3		
1-3B	33.3		112.1
2-4		53.0	
<b>Compression</b>			
1-3A	156.5		
2-5		112.5	71.9
1-6	214.0		
1-9		168.5	78.7
Stiffness (tons/in)			
<b>Tension</b>			
1-2	125		
1-3B	160		174.7
2-4		249	
<b>Compression</b>			
1-3A	477		
2-5		580	121.6
1-6	448		
1-9		553	123.4

for the battered piles was 24.7% lower on the average than the allowable load for the vertical piles. The stiffness of the battered piles was 74.4% higher in tension and 22.5% higher in compression than the vertical piles.

3.5.5 Effect of Load Test Procedure. A comparison of allowable loads and stiffnesses for Standard versus Quick load test procedures is shown in Table 7. The piles were compared only if their length and batter were similar. It can be seen that the Quick test resulted in higher allowable loads than the Standard test in every case. The allowable loads for the Quick tests were 64.8% higher in tension and 43.3% higher in compression than the Standard tests. The stiffnesses of the Quick tests were 105.8% higher in tension and 5.3% lower in compression than the Standard tests.

Table 7. Comparison of Standard and Quick Test Procedures

File	Standard	Quick	Quick/Standard (%)
Allowable Load (tons)			
<b>Tension</b>			
1-2	61.3		
1-3B	33.4		143.6
2-1		68.0	
2-8	25.0		
3-15		45.0	186.0
3-16		48.0	
<b>Compression</b>			
1-3A	156.5		
1-6		214.0	136.7
2-5	112.5		
1-9		168.5	149.8
Stiffness (tons/in)			
<b>Tension</b>			
1-2	125		
1-3B	160		282.6
2-1		403	
2-8	357		
3-15		427	128.9
3-16		494	
<b>Compression</b>			
1-3A	477		
1-6		448	93.9
2-5	580		
1-9		553	95.3

3.5.6 Variability Across The Site. The variability of pile capacity across the site can be seen from Figures 15 through 20. Out of the 28 piles only two sets of two piles each could be found with similar length, batter and load test procedure. These sets are piles 1-2 and 1-3B and piles 3-15 and 3-16. The allowable loads on these two sets vary by 84% and 6% respectively, and the stiffnesses vary by 22% and 14% respectively. This variability in pile capacity, coupled with the soil variability shown in previous sections, points out the need to include the concepts of statistical distribution and probability of failure in a capacity prediction method. This would then allow the engineer to use a

factor of safety which results in an acceptable level of risk.

### 3.6 Load Transfer Curves

Under a compression load, a pile develops resistance from friction along the side of the pile and from bearing at the point of the pile. In an instrumented load test these components can be separated and be plotted versus the pile movement to result in load transfer curves. Four of the H-piles were tested in compression and were pushed far enough to fail the piles: piles 1-3A, 1-6, 1-9 and 2-5. The point load transfer curves are shown in Figure 25 and the average side load transfer curves are shown in Figure 26.

These transfer curves can be modelled by a linear elastic-plastic model which requires two parameters: an ultimate resistance - given by the peak of the transfer curve, and a quake - given by the movement required to reach the peak value. If the pile is pushed far enough during a load test, the ultimate resistance is obtained when the transfer curves reach a constant load with increasing movement. However, the value of the quake depends on what secant is drawn through the curve. An illustration of a 25% secant quake is shown in Figure 27. The secant is drawn through the curve at 25% of the ultimate resistance. Values of 25% and 50% secant quakes for the four piles are shown in Table 8.

Table 8. Measured Quake Values

Pile	50% Secant Quakes		25% Secant Quakes	
	Point (in.)	Side (in.)	Point (in.)	Side (in.)
1-3A	0.57	0.40	0.20	0.12
1-6	0.40	(0.35)	0.24	(0.45)
1-9	0.33	0.30	0.17	0.13
2-5	0.28	0.20	0.13	0.08
Average	0.40	0.30	0.19	0.11

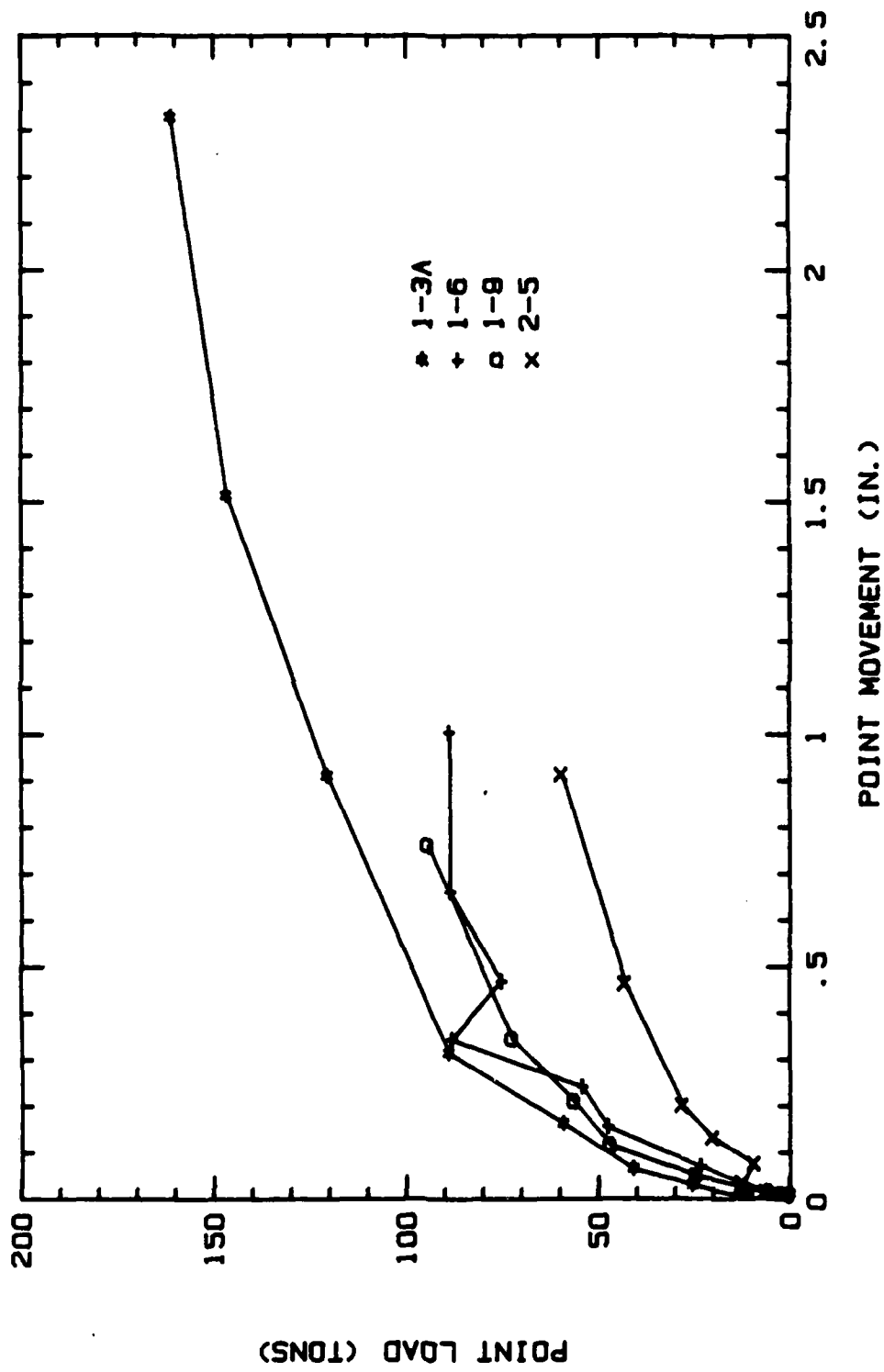


FIG. 25. Point Load Transfer Curves for H-Piles

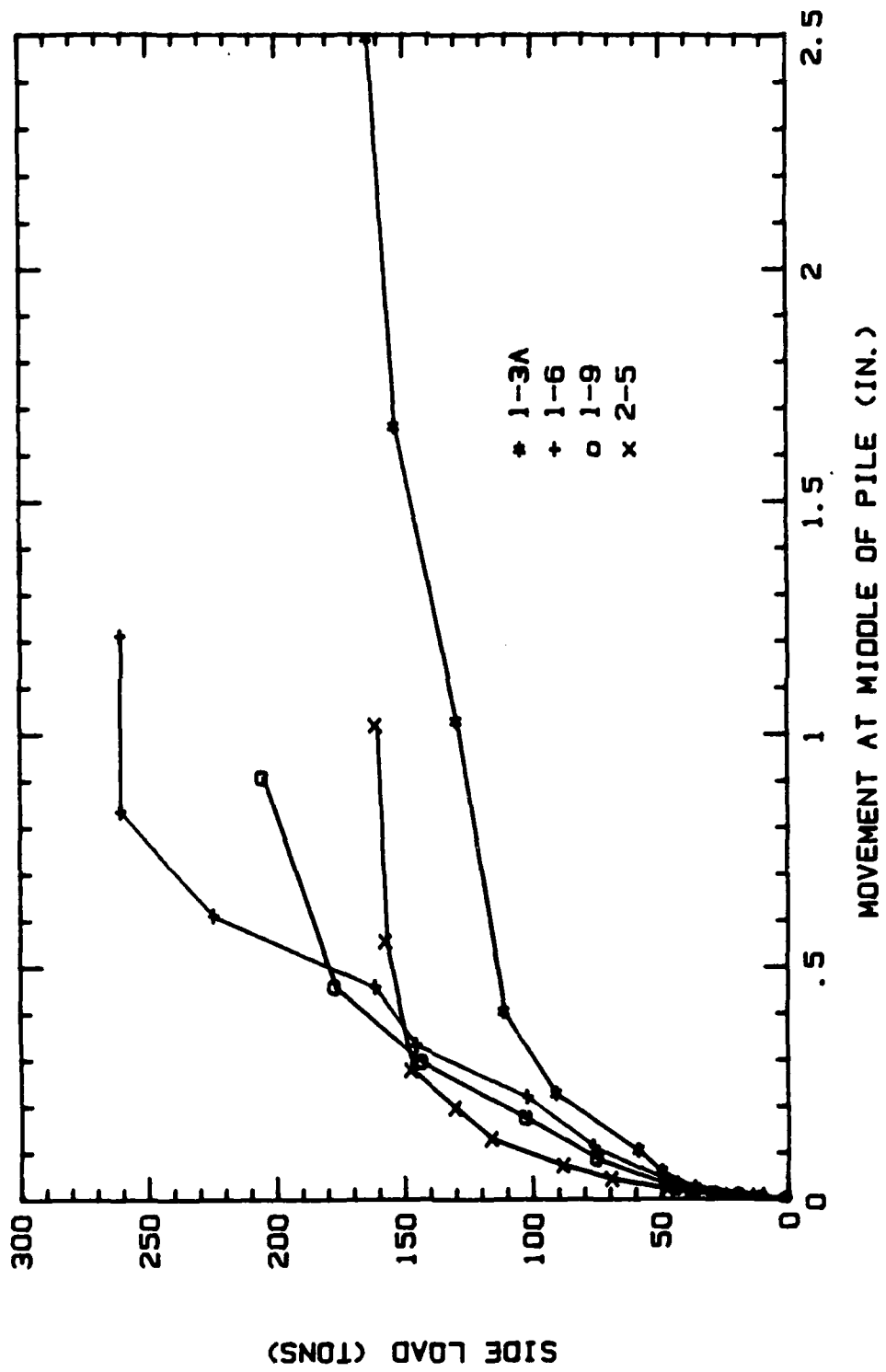


FIG. 26. Average Side Load Transfer Curves for H-Piles

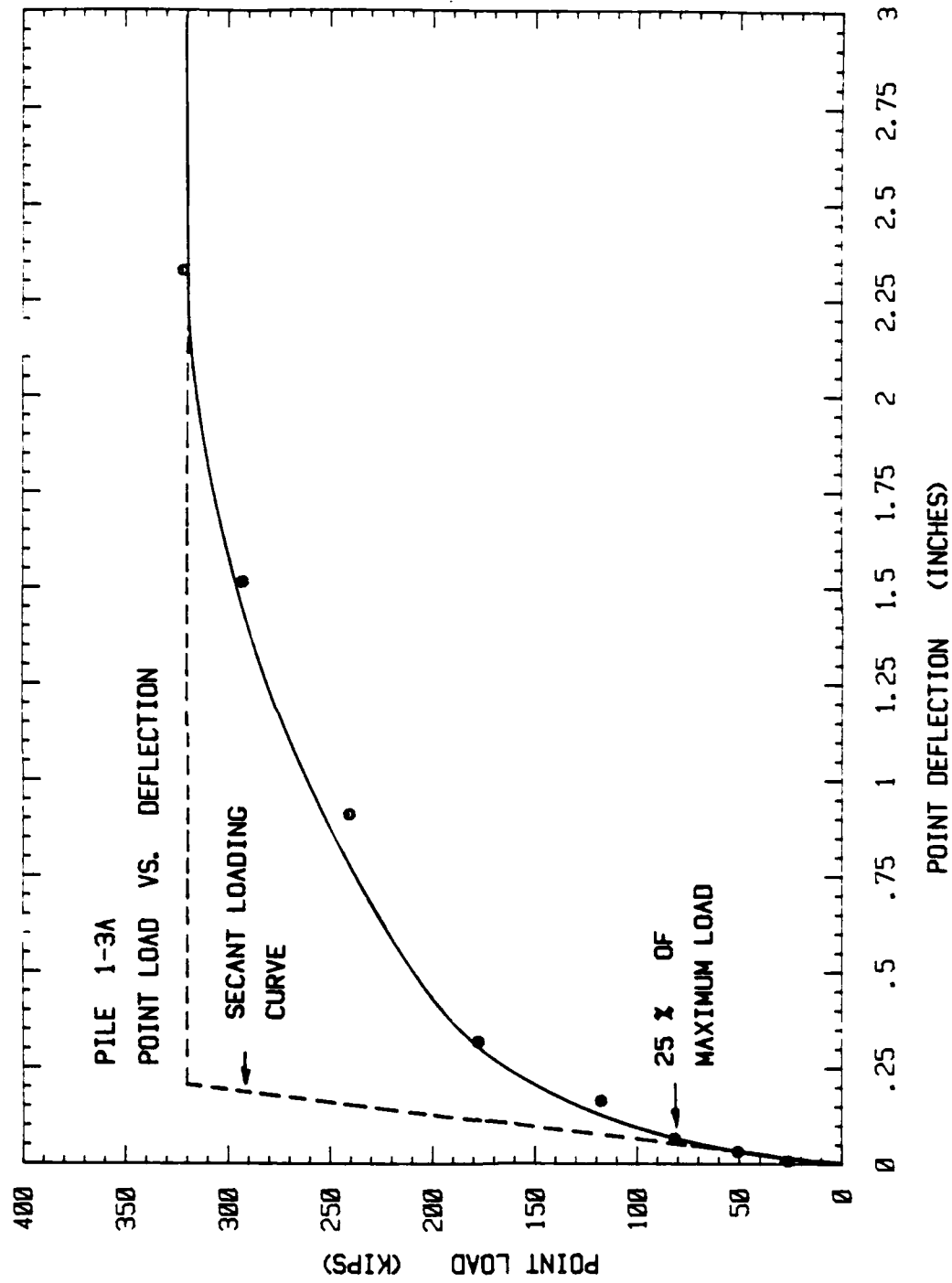


FIG. 27. Determination of 25% Secant Quake Values

#### 4. PREDICTED AXIAL PILE RESPONSE

##### 4.1 Pile Driving Analysis

4.1.1 Pile Driving Analyzer. Dynamic field measurements made using the Pile Driving Analyzer Model GA developed by Goble were made available for four piles: piles 1-3A, 1-6, 1-9 and 2-5. The parameters obtained are

FMAX, the maximum measured compression force at the transducer location, kips.

RSTC, the Case-Goble method static resistance using damping (J), kips.

EMAX, the maximum value of energy transmitted past the transducer location, kip-feet.

RMAX, the maximum Case-Goble method resistance using damping, kips.

The average values of these parameters for the last foot of penetration during initial driving are given in Table 9. The Case-Goble method has been calibrated to ultimate loads given by Davisson's failure criterion (Peck et al., 1974). The ultimate loads given by this criterion are shown in Table 9 for comparison. It can be seen that the value of RSTC averages 58% of the ultimate load measured in the load test, and RMAX averages 66% of the ultimate load measured in the load test. This indicates that the damping value, J, used in the Case-Goble method was too high or that the pile gained capacity between the end of driving and the time of the load test.

4.1.2 Wave Equation Analysis. A wave equation analysis was performed for the four H-piles for which load transfer curves were available (Briaud et al., 1984). The analysis was performed using the program TIDYWAVE (Lowery, 1982), and used a multiple blow option to account



Table 9. Pile Driving Analyzer Measurements

File	FMAX (kips)	RSTC (kips)	EMAX (kip-ft)	RMAX (kips)	Ultimate Load Davisson Crit. (kips)
1-3A	590	367	13.8	372	450
1-6	465	388	26.4	391	600
1-9	473	240	NA	304	560
2-5	469	173	10.6	244	400

for residual driving stress effects. An analysis of pile 1-3A using the measured quakes presented in Section 3.6 showed that the 25% secant quakes produced better correlation with measured results. Bearing graphs were developed for piles 1-3A, 1-9 and 2-5 using damping values of:

$$J_{\text{point}} = 0.00 \text{ sec/ft}$$

$$0.05 \text{ sec/ft}$$

$$0.15 \text{ sec/ft}$$

$$0.30 \text{ sec/ft}$$

$$J_{\text{side}} = 1/3 J_{\text{point}}$$

The results are shown in Figures 28, 29 and 30. The results for pile 1-6 were unusual because of its comparatively high static soil resistance and its abnormally large side quake value. Due to the high side quake value the wave equation analysis showed the pile coming out of the ground with each blow instead of penetrating. Therefore, the results of this pile are not reported. Figures 28 through 30 show that a damping value of 0.0 yields the closest results to the measured ultimate load from the load test, and that a negative damping value would be required to actually match the measured results. The low predicted resistances could be attributed to soil setup. However, the piles would have to experience a 67% gain in strength in order for the predictions to match

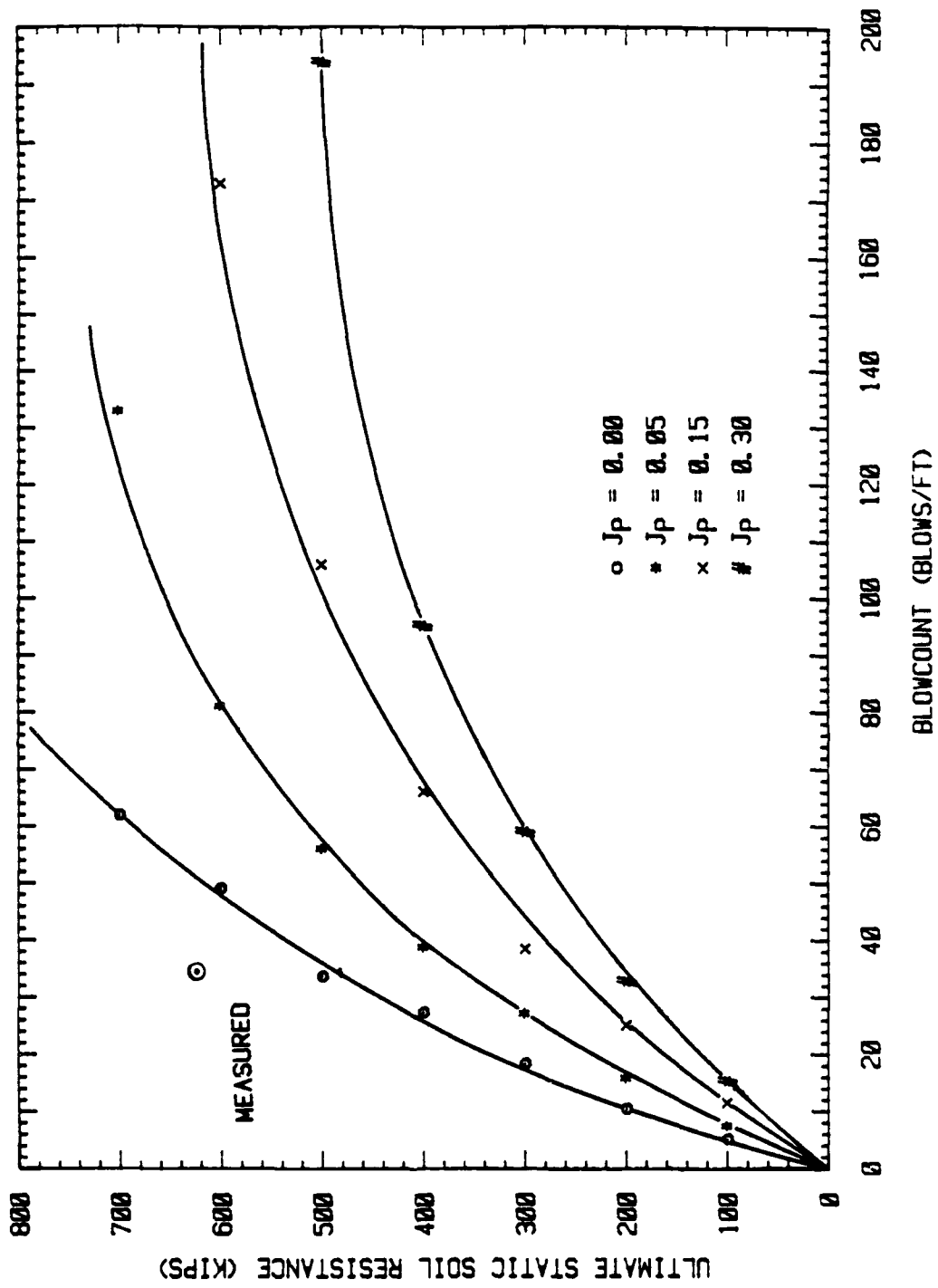


FIG. 28. RUT Versus N for Pile 1-3A Using 25% Secant Quakes

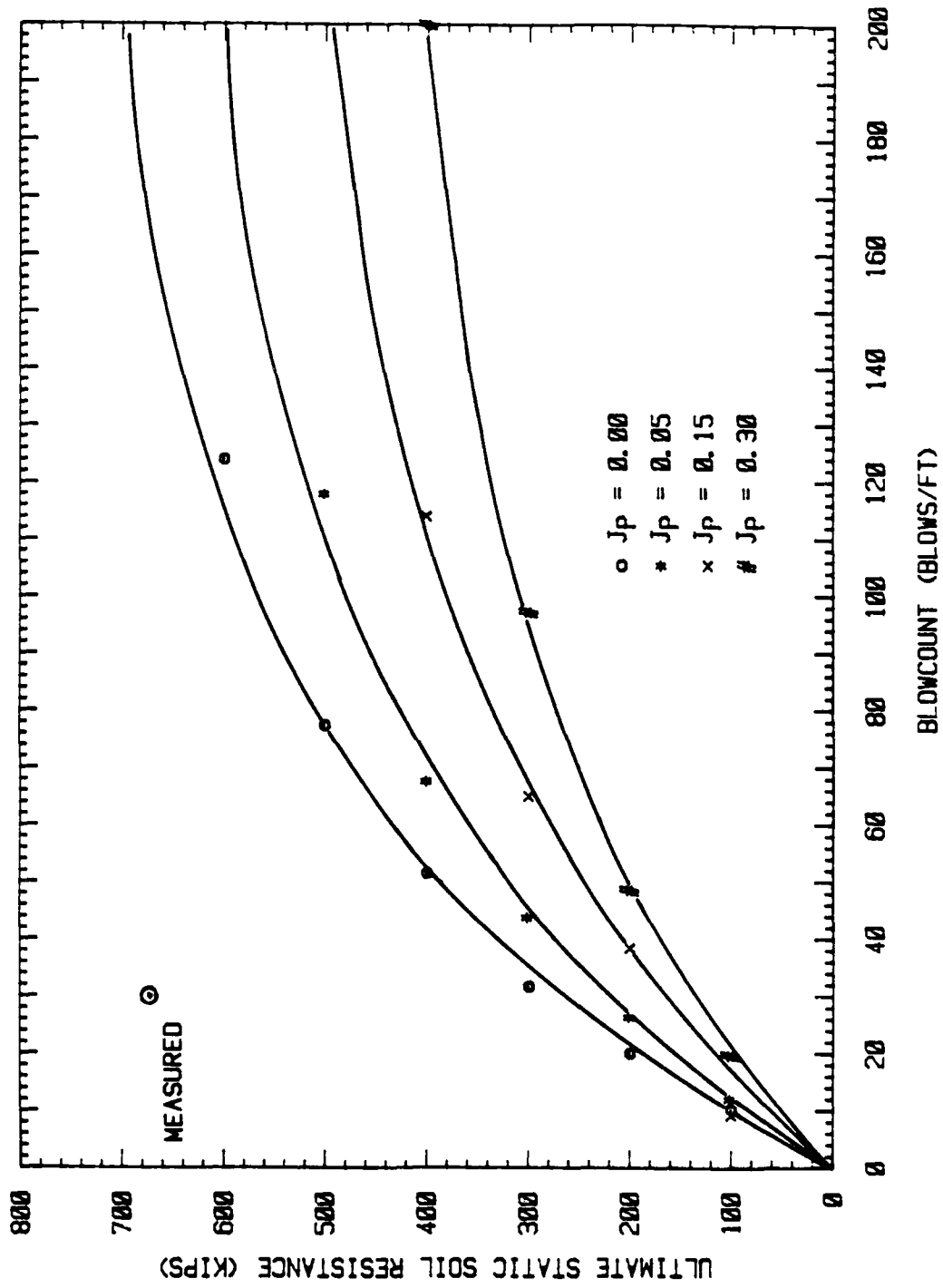


FIG. 29. RUT Versus N for Pile 1-9 Using 25% Secant Quakes

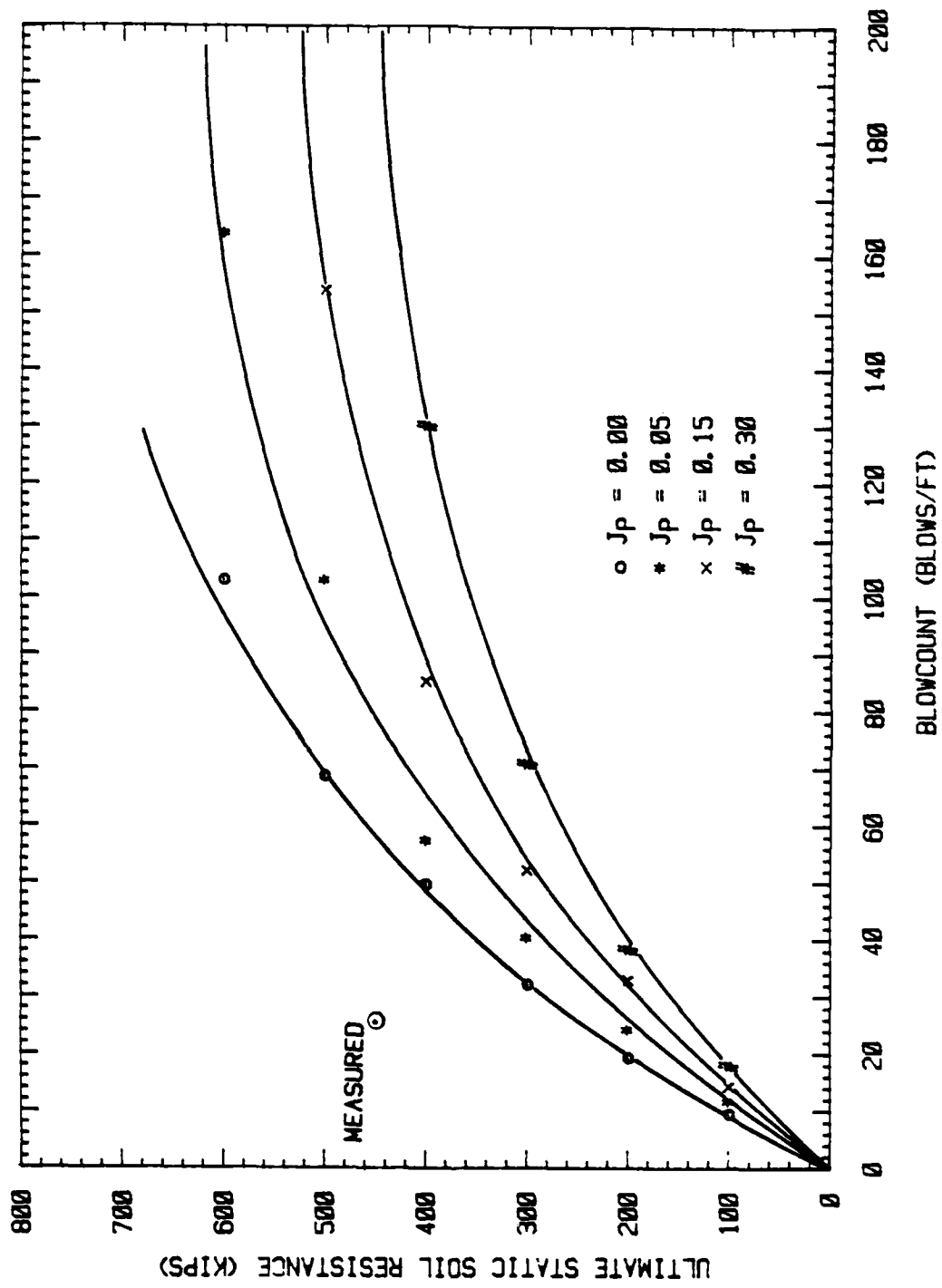


FIG. 30. RUT Versus N for Pile 2-5 Using 25% Secant Quakes

the measured resistances, which would be unusual in a medium to coarse relatively clean sand (7% < #200 sieve).

**4.1.3 Engineering News Formula.** The Engineering News Formula (ENF) is one of the most widely used dynamic formulas for determining pile capacity at the time of driving. For double-acting diesel hammers the formula is as follows:

$$Q = \frac{2 E}{S + 0.1"}$$

where Q = allowable load, kips

E = rated energy, kip-ft

S = average pile set during the last foot of penetration, inches.

The results are shown in Table 10 for the seven piles tested in compression which reached failure and are compared to the measured allowable load assuming a factor of safety of two. Table 11 shows the mean, standard deviation and coefficient of variation of the ratio of predicted over measured allowable load. These parameters are shown for H-piles, pipe piles and overall. In general the ENF is very conservative. It can be seen that the formula is more conservative for the H-piles than

Table 10. Engineering News Formula Predictions

Pile	Average Blowcount (blows/ft)	Predicted Allowable Load (kips)	Measured Allowable Load (kips)
1-3A	31	164	313
1-6	38	192	428
1-9	29	156	337
2-5	24	133	225
3-1	13	78	132
3-4	28	151	130
3-7	22	124	183

Table 11. Statistical Analysis of ENF Predictions

	Mean	Standard Deviation	Coefficient of Variation	Number of Items
H-piles	0.51	0.07	0.13	4
Pipe piles	0.81	0.31	0.38	3
Overall	0.64	0.24	0.38	7

for pipe piles. However, there is more scatter in the predictions for the pipe piles than for the H-piles.

#### 4.2 Static Capacity Prediction Methods

The static capacities of the tested piles were predicted by various methods based on the in situ test results presented in Section 2.2. Eight methods were used to predict pile capacities, with four methods using SPT data, three methods using CPT data and one method using PMT data. Table 12 shows the soil data needed for the eight methods and the references where details of the methods can be found.

The soil data used in the predictions was taken from the closest boring to the respective pile group. In the case of the CPT tests, boring B22 in pile group 2 and boring 5C in pile group 3 did not reach a sufficient depth to predict the pile capacities. In these two cases the CPT data was completed by using boring 6A which was located outside pile group 3. The values for the pressuremeter parameters for each pile group were an average of the data available at each group. These values are shown in Figures 10 through 12. The soil data used in the predictions for each pile group are summarized in Table 13. None of the methods made any recommendations for change in pile capacity due to rate of loading or due to pile batter.

Table 12. Summary of Prediction Methods

Method	Reference	Soil Data Used
Coyle	Coyle and Castello 1981	SPT
Briaud/Tucker	Briaud and Tucker 1984	SPT
Meyerhof	Meyerhof 1976	SPT
A.P.I.	A.P.I. 1984	SPT
Laboratoire des Ponts et Chaussees (LPC)		
Briaud et al.	Briaud et al. 1985	CPT
deRuiter/Beringen	deRuiter and Beringen 1979	CPT
Schmertmann	Schmertmann 1978	CPT
L.P.C.	Briaud et al. 1985	PMT

Table 13. Summary of Soil Borings Used for Predictions

Pile Group	Boring		
	SPT	CPT	PMT
1	B19	B12	see Fig. 8
2	B21	B22 + B6A	see Fig. 9
3	B20	B5C + B6A	see Fig. 10

#### 4.3 Comparison of Predicted and Measured Results

The predicted and measured ultimate loads for eight H-piles and three pipe piles loaded in tension are shown in Table 14. The predictions for the H-piles loaded in tension assumed that the piles were fully plugged between the flanges. This assumption produces the smallest perimeter and therefore the smallest predicted capacity.

The predicted and measured ultimate loads for three H-piles and three pipe piles loaded in compression are shown in Table 15. The predictions of the ultimate load for the H-piles have been made using three assumptions. First, the capacities were predicted assuming that the piles were fully plugged between the flanges. Second, the capacities were predicted assuming that the piles were unplugged, so that the piles

Table 14. Predicted and Measured Ultimate Loads in Tension

File No.	1-2	1-3B	2-1	2-3	2-4	2-8	3-2	3-5	3-8	3-15	3-16
Method	Load (kips)										
Coyle	332	332	362	490	389	229	139	158	171	207	207
Briaud/Tucker	311	311	336	446	359	222	131	155	177	202	202
Meyerhof	331	331	406	618	449	214	121	144	164	187	187
A.P.I.	222	222	232	392	266	106	59	71	81	93	93
L.P.C. CPT	301	301	348	438	368	251	149	176	201	229	229
deRuiter/Beringen	149	149	243	317	262	161	101	121	136	158	158
Schmertmann	487	487	467	555	484	324	99	116	131	171	171
L.P.C. PMT	446	446	446	606	496	319	166	197	150	248	248
Measured	245	133	272	312	212	100	122	137	200	180	192

failed along the actual steel-soil interface around the pile. The third assumption was that the piles were half-plugged, which is the average of the first two cases.

In an effort to quantify which method performed the best, a statistical analysis was performed of the ratio of the predicted over the measured ultimate load. The mean, standard deviation and coefficient of variation of this ratio is shown in Table 16 for the tension tests and in Tables 17 through 20 for the compression tests. The ratios were computed for point load, side load and total load for the H-piles tested in compression. A perfect prediction method would have a mean of one, a standard deviation of zero and a coefficient of variation of zero.

#### 4.4 Discussion of the Results

The statistical analysis of the tension tests shows that, for the H-piles, the A.P.I. method was the best SPT method and the deRuiter/Beringen method was the best CPT method. For the pipe piles in



Table 15. Predicted and Measured Ultimate Loads in Compression

Method	1-3A			1-6			2-5			3-1			3-4			3-7		
	Q <sub>p</sub>	Q <sub>s</sub> (kips)	Q <sub>t</sub>	Q <sub>p</sub>	Q <sub>s</sub> (kips)	Q <sub>t</sub>	Q <sub>p</sub>	Q <sub>s</sub> (kips)	Q <sub>t</sub>	Q <sub>p</sub>	Q <sub>s</sub> (kips)	Q <sub>t</sub>	Q <sub>p</sub>	Q <sub>s</sub> (kips)	Q <sub>t</sub>	Q <sub>p</sub>	Q <sub>s</sub> (kips)	Q <sub>t</sub>
<b>Plugged</b>																		
Coyle	345	332	677	345	323	668	345	398	743	196	204	400	267	233	500	349	262	611
Briaud/Tucker	242	311	553	240	304	544	260	366	626	127	180	307	171	212	383	223	246	469
Meyerhof	586	331	917	581	319	900	677	460	1137	191	278	469	369	225	594	479	261	740
A.P.I.	221	222	443	216	211	427	249	277	526	87	110	197	120	132	252	159	154	313
L.P.C. CPT	217	307	524	205	301	506	276	375	651	155	197	352	208	232	440	226	269	495
deRuiter/Beringen	432	194	626	432	189	621	432	333	765	246	190	436	335	192	527	437	261	698
Schmertmann	484	478	962	478	463	941	755	489	1244	367	161	528	369	157	526	615	218	833
L.P.C. FMT	116	446	562	116	435	551	109	505	614	56	102	158	77	139	216	100	162	262
<b>Unplugged</b>																		
Coyle	49	539	588	49	524	573	49	645	694									
Briaud/Tucker	34	504	538	34	492	526	37	598	635									
Meyerhof	83	537	620	82	517	598	96	753	849									
A.P.I.	31	359	390	31	342	373	35	454	489									
L.P.C. CPT	31	498	529	29	488	517	39	608	647									
deRuiter/Beringen	61	314	375	61	306	367	61	544	605									
Schmertmann	69	755	824	68	751	819	107	793	900									
L.P.C. FMT	17	721	738	16	705	721	17	820	837									
<b>Average of Plugged and Unplugged</b>																		
Coyle	197	435	632	197	423	620	197	521	718									
Briaud/Tucker	138	407	545	137	398	535	148	482	630									
Meyerhof	334	434	768	331	418	749	386	607	993									
A.P.I.	126	290	416	123	277	400	142	365	507									
L.P.C. CPT	124	402	526	117	394	511	157	492	649									
deRuiter/Beringen	246	254	500	246	248	494	246	439	685									
Schmertmann	276	617	893	273	607	880	431	641	1072									
L.P.C. FMT	66	584	650	66	570	636	63	662	725									
Measured	304	322	626	152	704	856	92	358	450	---	---	264	---	---	260	---	---	366

Table 16. Statistical Analysis of Tension Tests

Method	H-Piles			Pipe Piles		
	Mean	Standard Deviation	Coefficient of Variation	Mean	Standard Deviation	Coefficient of Variation
Coyle	1.64	0.53	0.32	1.05	0.17	0.16
Briaud/Tucker	1.55	0.49	0.32	1.03	0.13	0.13
Meyerhof	1.70	0.56	0.33	0.95	0.12	0.13
A.P.I.	1.00	0.40	0.40	0.47	0.06	0.12
L.P.C. CPT	1.61	0.51	0.32	1.17	0.15	0.13
deRuiter/Beringen	1.02	0.30	0.30	0.80	0.11	0.13
Schmertmann	2.06	0.99	0.48	0.77	0.10	0.13
L.P.C. FMT	2.12	0.78	0.37	1.18	0.38	0.32

Table 17. Statistical Analysis of Compression Tests on H-Piles - Plugged Case

Method	Point Load			Side Load			Total Load		
	Mean	Standard Deviation	Coefficient of Variation	Mean	Standard Deviation	Coefficient of Variation	Mean	Standard Deviation	Coefficient of Variation
Coyle	2.38	1.31	0.55	0.87	0.36	0.41	1.17	0.44	0.38
Briaud/Tucker	1.73	1.02	0.59	0.81	0.32	0.40	0.97	0.39	0.40
Meyerhof	4.37	2.76	0.63	0.92	0.43	0.46	1.68	0.76	0.45
A.P.I.	1.62	1.00	0.62	0.59	0.25	0.43	0.79	0.34	0.43
L.P.C. CPT	1.69	1.18	0.70	0.81	0.33	0.41	0.96	0.44	0.46
deRuiter/Beringen	2.99	1.64	0.55	0.60	0.33	0.55	1.14	0.50	0.44
Schmertmann	4.31	3.46	0.80	1.17	0.45	0.38	1.80	0.86	0.48
L.P.C. PMT	0.78	0.40	0.52	1.14	0.45	0.40	0.97	0.37	0.38

Table 18. Statistical Analysis of Compression Tests on H-Piles - Unplugged Case

Method	Point Load			Side Load			Total Load		
	Mean	Standard Deviation	Coefficient of Variation	Mean	Standard Deviation	Coefficient of Variation	Mean	Standard Deviation	Coefficient of Variation
Coyle	0.34	0.19	0.55	1.41	0.58	0.41	1.05	0.45	0.43
Briaud/Tucker	0.25	0.15	0.60	1.31	0.53	0.41	0.96	0.41	0.42
Meyerhof	0.62	0.39	0.63	1.50	0.70	0.47	1.19	0.62	0.52
A.P.I.	0.23	0.14	0.62	0.96	0.41	0.43	0.72	0.34	0.47
L.P.C. CPT	0.23	0.14	0.62	1.31	0.54	0.41	0.96	0.43	0.45
deRuiter/Beringen	0.42	0.23	0.55	0.98	0.54	0.56	0.79	0.49	0.62
Schmertmann	0.61	0.49	0.80	1.88	0.70	0.38	1.42	0.53	0.37
L.P.C. PMT	0.12	0.07	0.56	1.84	0.73	0.40	1.29	0.52	0.40

Table 19. Statistical Analysis of Compression Tests on H-Piles - Half-plugged Case

Method	Point Load			Side Load			Total Load		
	Mean	Standard Deviation	Coefficient of Variation	Mean	Standard Deviation	Coefficient of Variation	Mean	Standard Deviation	Coefficient of Variation
Coyle	1.36	0.75	0.55	1.14	0.47	0.41	1.11	0.44	0.40
Briaud/Tucker	0.99	0.59	0.59	1.06	0.43	0.41	0.97	0.40	0.41
Meyerhof	2.49	1.57	0.63	1.21	0.56	0.46	1.44	0.69	0.48
A.P.I.	0.92	0.57	0.62	0.77	0.33	0.43	0.75	0.34	0.45
L.P.C. CPT	0.96	0.67	0.70	1.06	0.44	0.41	0.96	0.43	0.45
deRuiter/Beringen	1.70	0.94	0.55	0.79	0.44	0.55	0.97	0.49	0.51
Schmertmann	2.46	1.97	0.80	1.59	0.45	0.28	1.61	0.70	0.43
L.P.C. PMT	0.45	0.23	0.52	1.49	0.59	0.40	1.13	0.44	0.39

Table 20. Statistical Analysis of Compression Tests of Pipe Piles

Method	Mean	Standard Deviation	Coefficient of Variation
Coyle	1.70	0.21	0.12
Briaud/Tucker	1.31	0.16	0.12
Meyerhof	2.03	0.25	0.13
A.P.I.	0.87	0.11	0.13
L.P.C. CPT	1.46	0.20	0.14
deRuiter/Beringen	1.86	0.19	10
Schmertmann	2.10	0.15	07
L.P.C. PMT	0.72	0.12	0.16

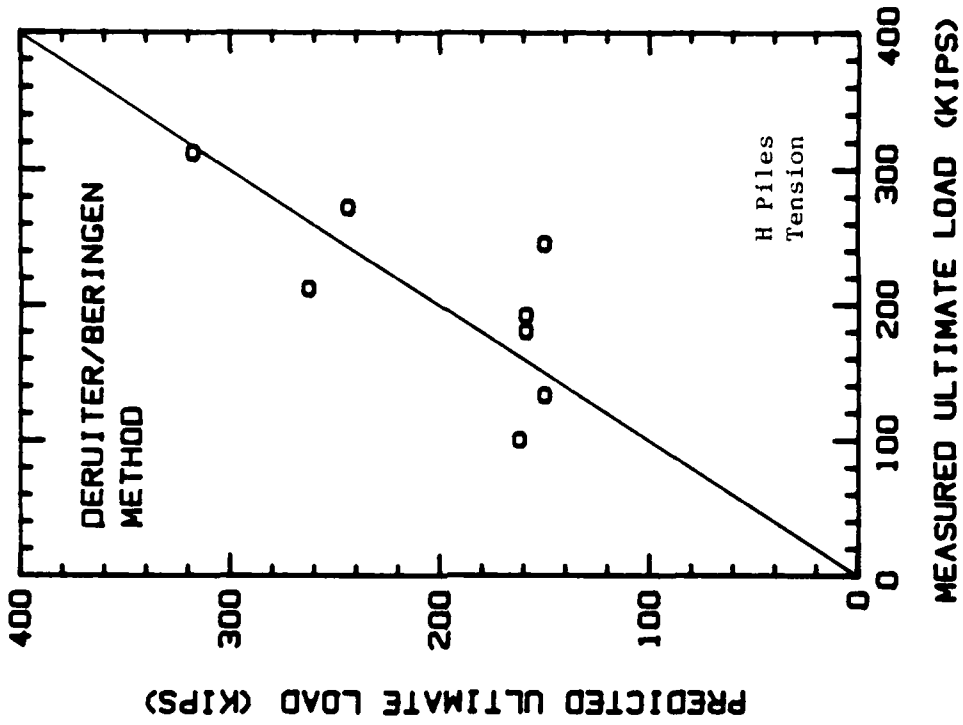
tension the Coyle, Briaud/Tucker and Meyerhof methods all predicted capacities very well using SPT data, and all three CPT methods ranked about the same.

In analyzing the H-pile compression tests it can be seen that, in general, the plugged, unplugged and half-plugged cases produced similar statistics for the total load for a given method. However, the plugged assumption generally led to an overestimation of the point load and underestimation of the side load. The unplugged assumption led to an underestimation of the point load and an overestimation of the side load. The half-plugged assumption gave the best results in terms of predicting not only ultimate load but also the value of the point load and of the side load. The Briaud/Tucker method was the best SPT method and the L.P.C. method was the best CPT method.

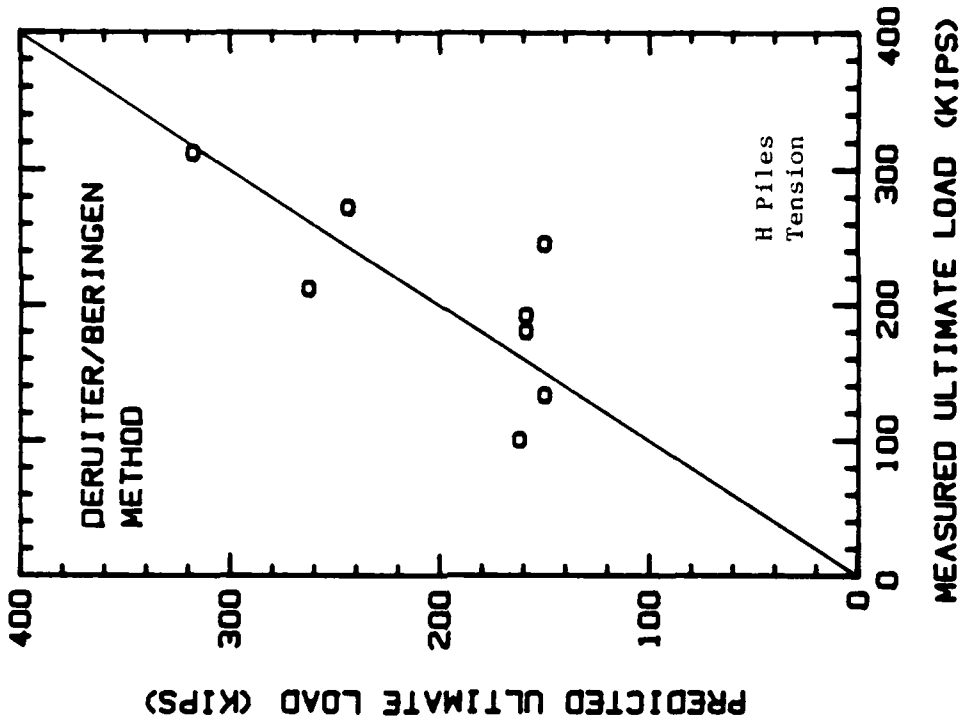
For the pipe piles in compression, most of the methods tended to overpredict the pile capacities. The A.P.I. method was the best SPT method and the L.P.C. method was the best CPT method. The predicted and

measured ultimate loads are compared in Figures 31 through 34 for the best prediction method in each category.

An interesting result of the statistical analysis is that the coefficient of variation for the pipe pile predictions is about one-third that of the H-pile predictions for the tension tests, and is about one-fourth that of the H-pile predictions for the compression tests. This indicates that the measured H-pile capacities varied much more than the measured pipe pile capacities. A possible cause of this may be cobbles or boulders being lodged in between the flanges of the H-piles or damaging the tips of the piles such as was observed by Fruco and Associates (1973) in a pile driveability study done in this same area. Since the pipe piles were driven closed-ended and to shallower depths than the H-piles these problems would not affect their capacities.

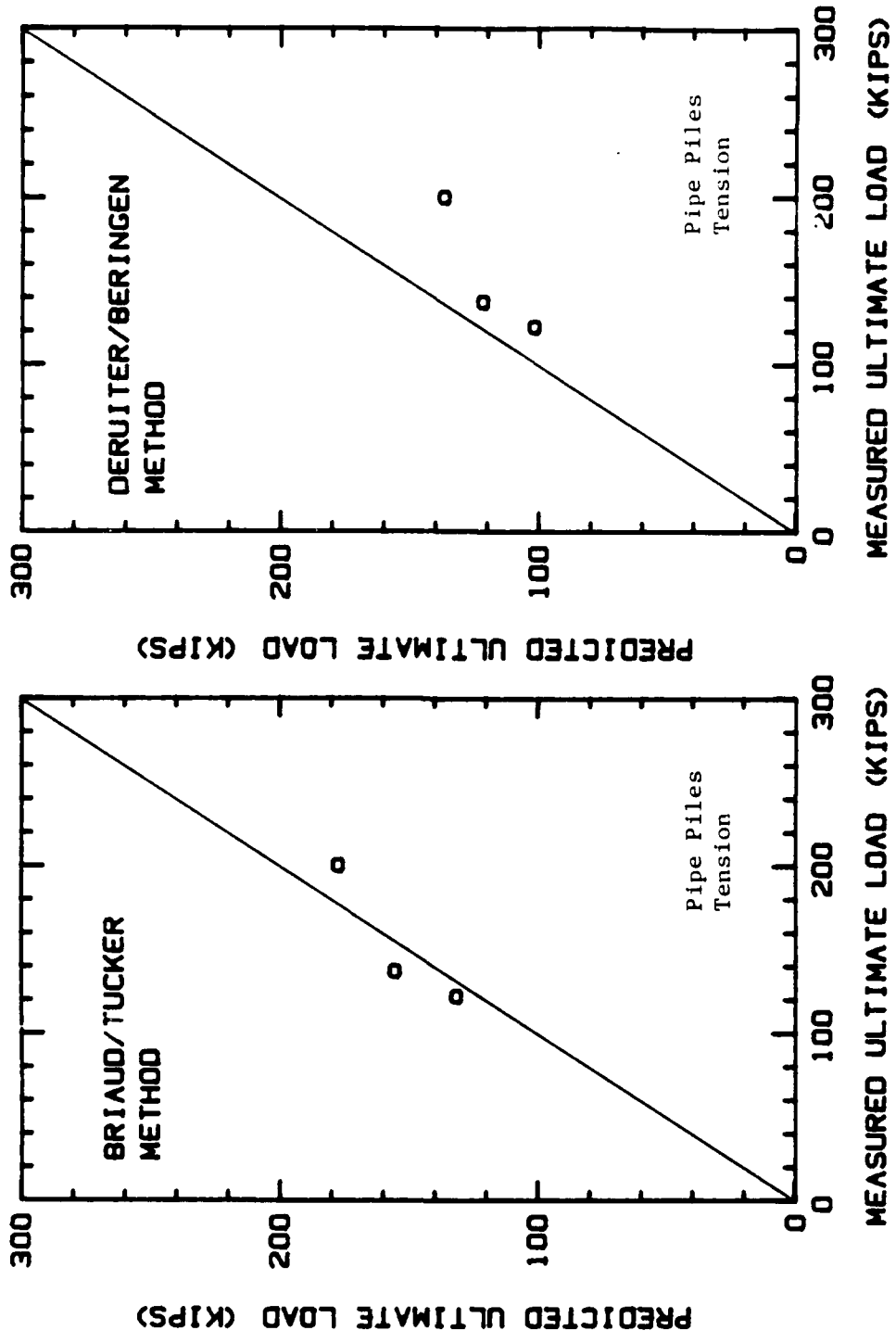


(a) Best SPT Method



(b) Best CPT Method

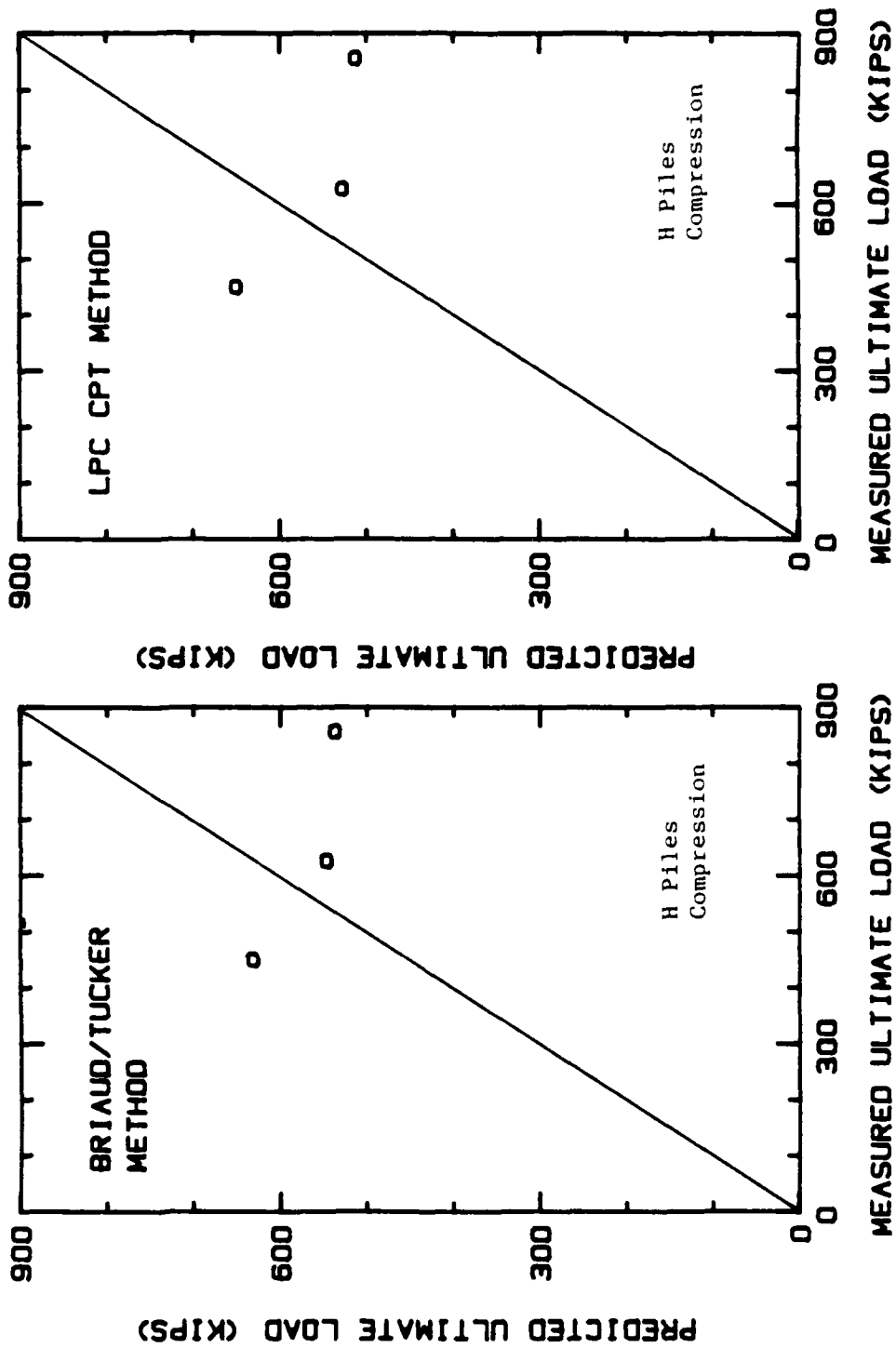
FIG. 31. Predicted Versus Measured Ultimate Loads for H-Piles in Tension



(a) Best SPT Method

(b) Best CPT Method

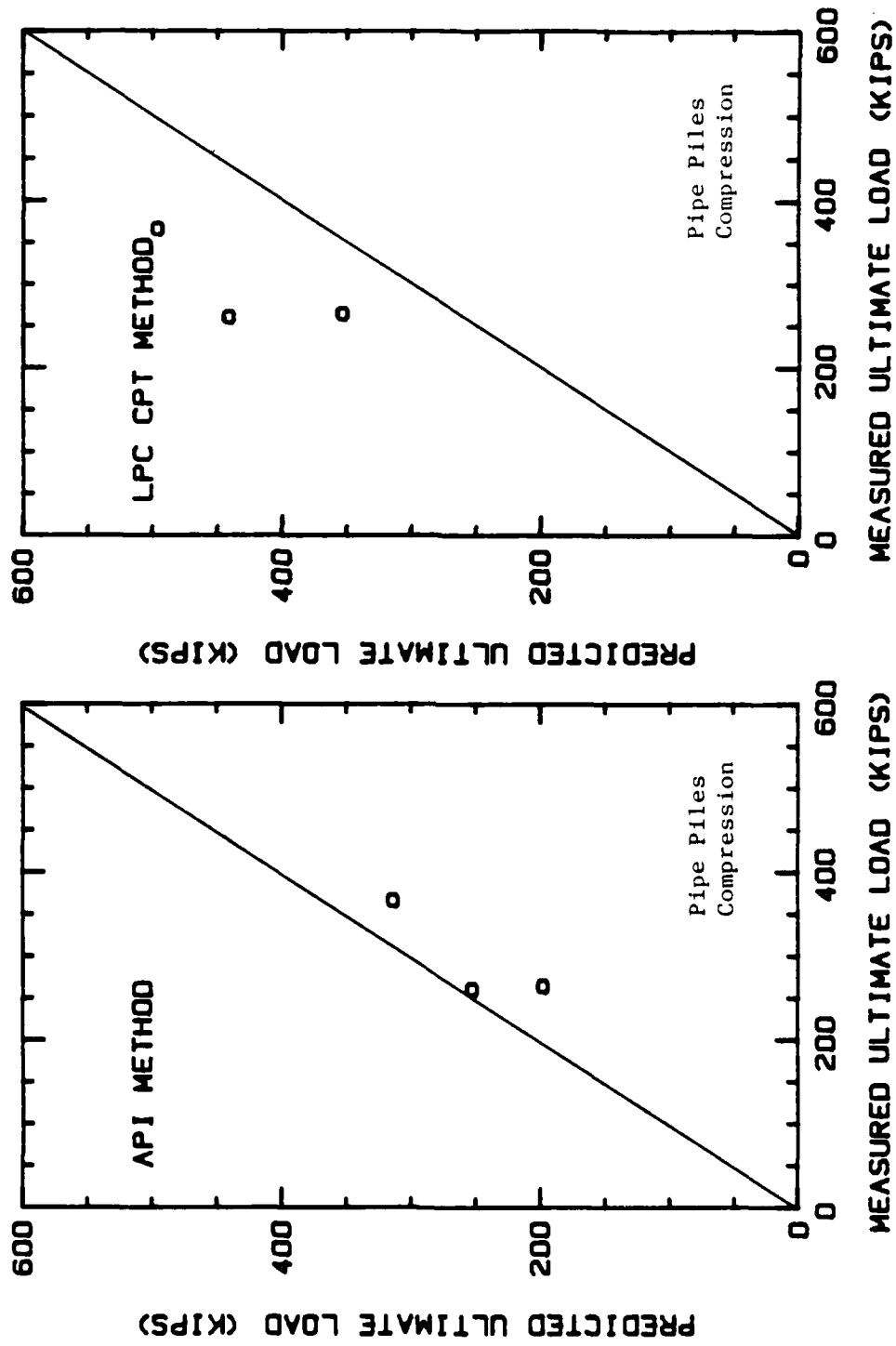
FIG. 32. Predicted Versus Measured Ultimate Loads for Pipe Piles in Tension



(a) Best SPT Method

(b) Best CPT Method

FIG. 33. Predicted Versus Measured Ultimate Loads for H-Piles in Compression



(a) Best SPT Method

(b) Best CPT Method

FIG. 34. Predicted Versus Measured Ultimate Loads for Pipe Piles in Compression



## 5. THE LATERAL LOAD TEST PROGRAM

### 5.1 The Load Test Program

Lateral load tests were performed on two H-piles with embedded lengths of 67 ft. The load test setup is shown in Figure 35. The two piles were jacked apart and the lateral displacement of each pile was measured. The loading schedule consisted of monotonic loading to 0.5 in. deflection, followed by 25 cycles from 0 to 14 tons, and then loading to 2 in. deflection. The load was applied 6.5 in. above the ground surface and the deflections were measured at that same point.

### 5.2 The Prediction Methods

The conventional P-y curves proposed by Reese et al. (1974), a subgrade reaction method (Broms 1964) and P-y curves derived from pressuremeter tests (Briaud et al. 1982) were used to predict the lateral load-deflection behavior of the H-piles.

Reese et al. define the soil resistance,  $P$ , as a function of the friction angle,  $\phi$ , the average effective unit weight of the soil, the pile width and the depth to the desired P-y curve. By calculating  $P$  and the associated deflection,  $y$ , of three defined points, the P-y curve can be determined at a given depth. Figure 36 shows sample P-y curves for varying depths,  $X$ . The initial linear portion of the P-y curve has a slope  $K_s X$ , where  $K_s$  is a constant ( $\text{lb/in}^3$ ) depending only upon the relative density of the sand. A  $K_s$  value of  $125 \text{ lb/in}^3$  (dense sand) was used for the predictions. Using this recommended  $K_s$  value the initial linear portion of the P-y curves at greater depths was not stiff enough to yield a smooth curve to point  $m$  as illustrated in Figure 36. In these cases, a straight line was assumed from the origin to point  $m$ . The parameters used in computing the P-y curves are given in Table 21.

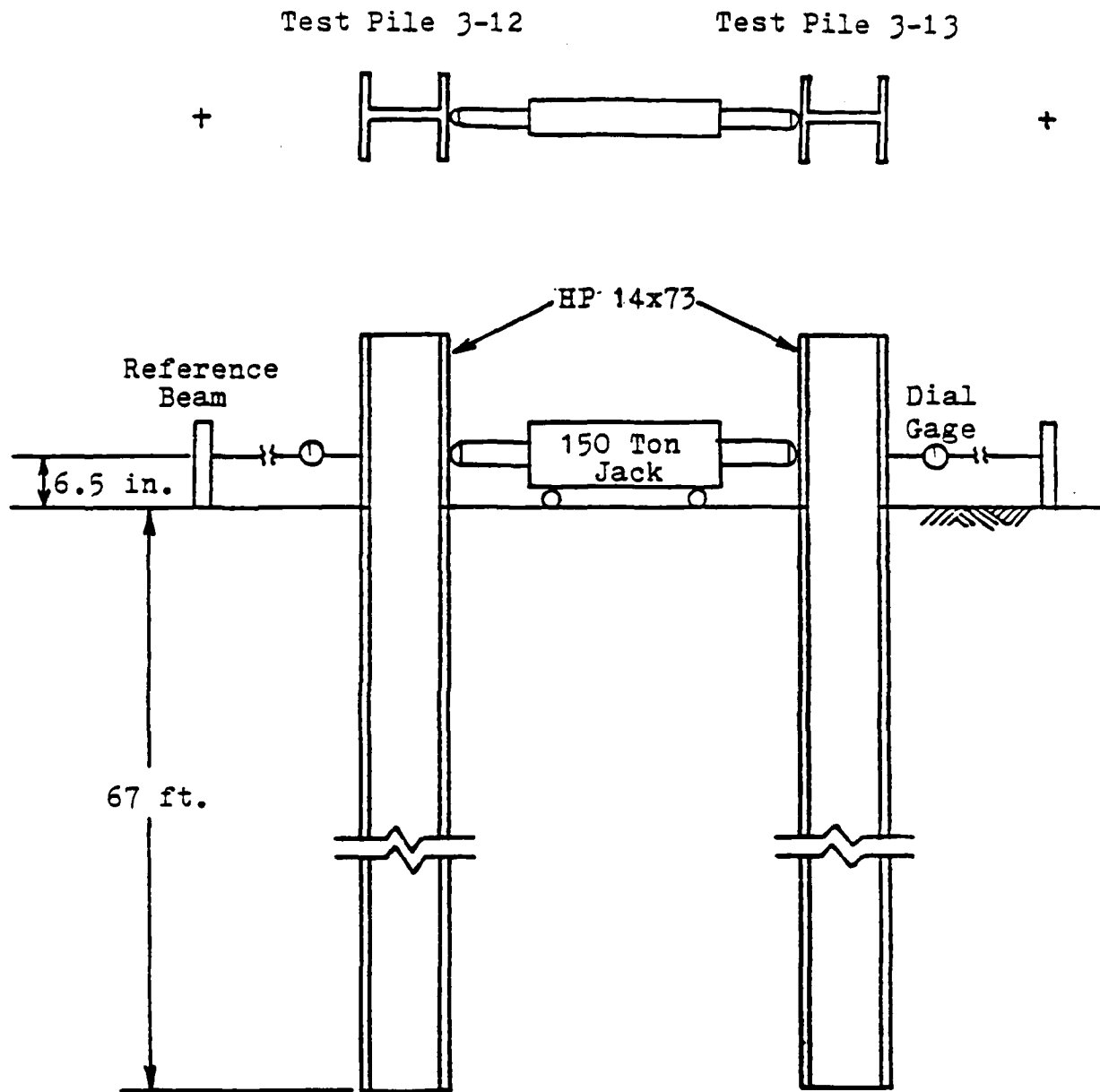


FIG. 35. Lateral Load Test Setup

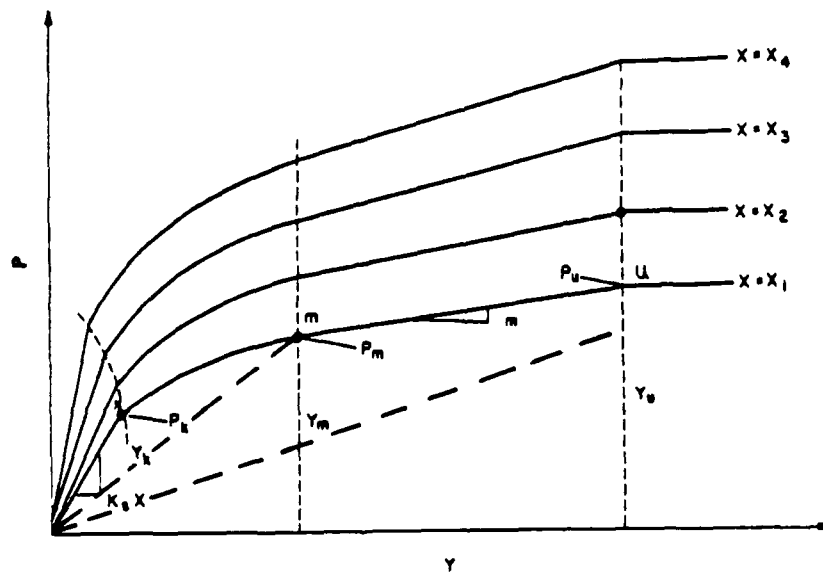


FIG. 36. Reese et al. P-y Curves in Sand  
(from Reese et al. 1974)

Table 21. Parameters Used for Reese et al. P-y Curves

Friction Angle	34° above 40 ft 42° below 40 ft
Total Unit Weight	116 lb/ft <sup>3</sup>

Broms' method for predicting deflections of a laterally loaded pile at working loads is based on the coefficient of lateral subgrade reaction (Broms 1964). The deflections of a free-head pile are computed from the following equation:

$$y = \frac{2.4 P}{n_h^{0.6} (EI)^{0.4}}$$

where  $n_h$  is the coefficient of horizontal subgrade reaction (lb/in<sup>3</sup>) for a long strip with a width of unity at a depth of unity below the ground surface, and EI is the pile stiffness. The recommended value  $n_h$  of 34 tons/ft<sup>3</sup> for dense sand below the water table was used for the predictions.

The method proposed by Briaud et al. (1982) for deriving P-y curves from pressuremeter data is based on the analogy of the laterally expanding pressuremeter probe to a laterally deflecting pile. The method considers that the lateral resistance has two components: friction and frontal resistance. This distinction is routinely made for the analysis of vertically loaded piles but has not been used for laterally loaded piles. Both the friction and frontal resistances are derived from the pressuremeter curve and are then added to obtain the P-y curve. The method has the advantage of using P-y curves which are measured in situ.

### 5.3 Comparison of Predicted and Measured Results

The predicted and measured load-deflection curves are shown in Figure 37. It can be seen that the Briaud et al. pressuremeter method predicts the measured data quite well. Broms' method also does well at working loads. The Reese et al. predictions are very conservative.

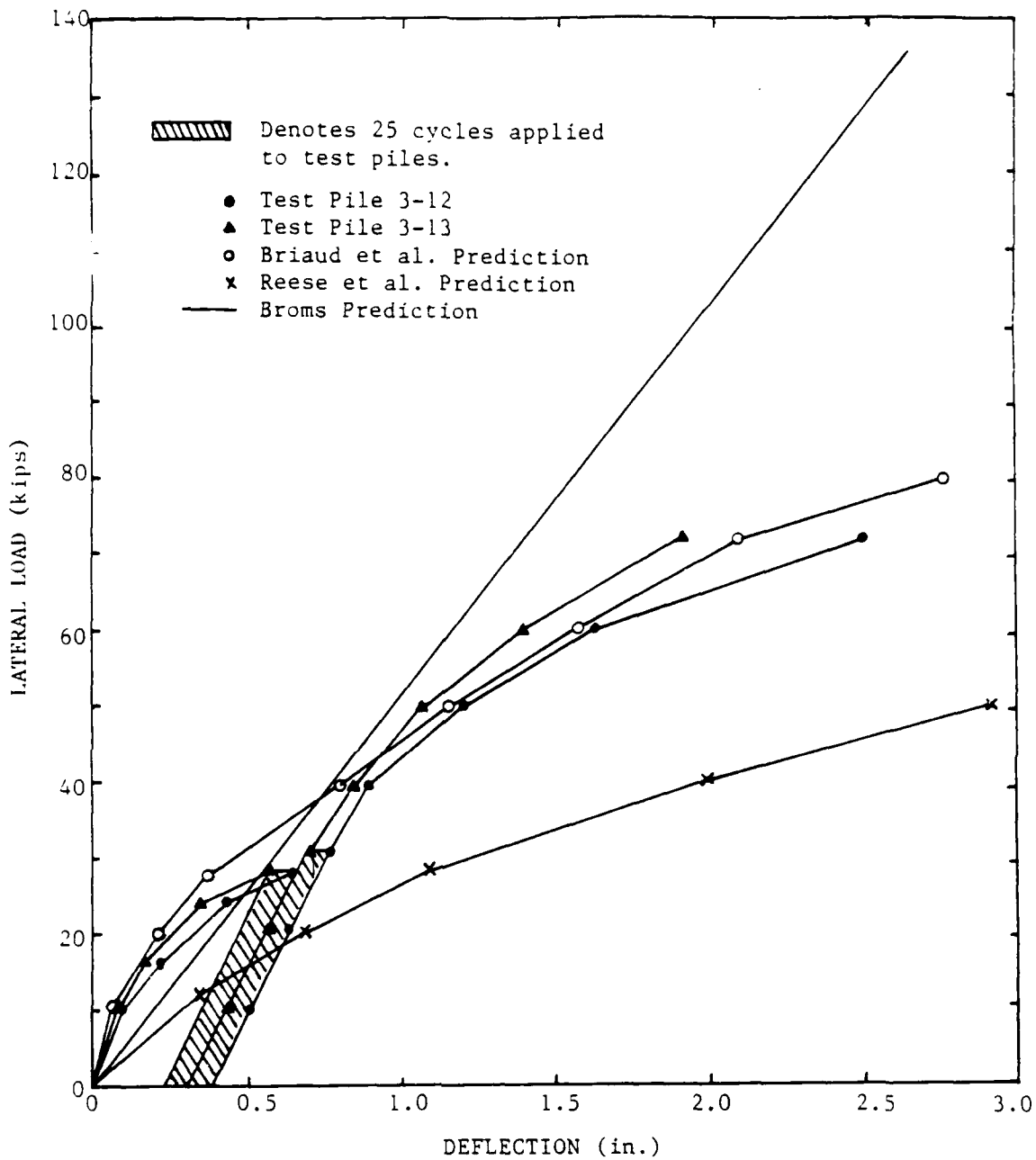


FIG. 37. Comparison of Predicted and Measured Lateral Deflections

## 6. CONCLUSIONS

The significant conclusions from this study can be summarized as follows:

1. Both dynamic capacity methods, the Engineering News Formula and the Case method, gave predicted ultimate loads which were much lower than the ultimate loads measured in the load tests. This may be due to soil setup, although unlikely in this relatively clean medium dense to dense sand and gravel.
2. A damping value of 0.0 was found to be the best value to use in a wave equation analysis to match measured results. This low damping value could explain why the Case prediction method was very conservative.
3. Residual point loads averaged 26.5 tons which is 30% of the average measured point load.
4. The settlements at working loads were small, however, the settlements of the H-piles averaged about three times those of the pipe piles in both tension and compression. This may be due to the larger volume of the displaced soil by the closed-ended pipe piles creating a denser surrounding soil.
5. The allowable load (factor of safety = 2) for battered H-piles was 12% higher in tension and 25% lower in compression than comparable vertical H-piles.
6. The initial stiffness of battered H-piles was 74% higher in tension and 23% higher in compression than comparable vertical H-piles.
7. The allowable load (factor of safety = 2) for Quick load tests on H-piles was 65% higher in tension and 43% higher in compression than comparable Standard load tests. This significant rate effect tends to make the soil "setup" mentioned in conclusion 1 more plausible.
8. The initial stiffness for Quick load tests on H-piles was 106% higher in tension and 5% lower in compression than comparable Standard load tests.
9. The allowable load on two similar piles in the same pile group varied as much as 84%. An analysis of 13 SPT borings showed an average coefficient of variation of 38%.
10. The friction on the H-piles in tension averaged 24% lower than the friction on the pipe piles in tension. This may be due to the fact that H piles are low displacement piles while the closed-ended pipe piles are large displacement piles.

11. The methods which best predicted the measured axial load capacities were:

		SPT	CPT
H-pile	Tension	A.P.I.	deRuiter/Beringen
H-pile	Comp.	Briaud/Tucker	deRuiter/Beringen
Pipe pile	Tension	Briaud/Tucker	L.P.C.
Pipe pile	Comp.	A.P.I.	L.P.C.

12. The capacity of an H-pile in tension should be calculated using the perimeter of the enclosing rectangle, as this will give the lowest predicted capacity. Most of the prediction methods still overestimated the pile capacity even using this perimeter.
13. The capacity of an H-pile in compression should be calculated assuming that the pile is half-plugged. This gives much better agreement with the measured point and side load distribution than either the full-plugged or unplugged assumption.
14. The Briaud et al. (1982) pressuremeter method gave the best predictions of the measured lateral load test results.



## 7. REFERENCES

- American Petroleum Institute, Recommended Practice for Planning, Designing, and Constructing Fixed Offshore Platforms, API-RP-2A, 1984.
- American Society for Testing and Materials, Annual Book of ASTM Standards, Part 19, Philadelphia, 1976.
- Briaud, J.-L., Brasuell, T.E., Tucker, L.M., "Case History of Two Laterally Loaded Piles at Lock & Dam 26 Replacement Site," Research Report 4690-3, Texas A&M University, 1984.
- Briaud, J.-L., Huff, L.G., Tucker, L.M., Coyle, H.M., "Evaluation of In Situ Tests Design Methods for Vertically Loaded H Piles at Lock and Dam No. 26 Replacement Dam," Research Report 4690-1, Texas A&M University, 1984.
- Briaud, J.-L., Lawson, W.D., Tucker, L.M., "Wave Equation Analysis for Piles in Gravel," Research Report 4690-2, Texas A&M University, 1984.
- Briaud, J.-L., Smith, T.D., Meyer, B.J., "Design of Laterally Loaded Piles Using Pressuremeter Tests Results," Symposium on the Pressuremeter and Its Marine Application, Paris, 1982.
- Briaud, J.-L., Tucker, L.M., "Coefficient of Variation of In Situ Tests in Sand," Proceedings, ASCE Symposium on Probabilistic Characterization of Soil Properties, Atlanta, 1984.
- Briaud, J.-L., Tucker, L.M., "Piles in Sand: A Method Including Residual Stresses," Journal of Geotechnical Engineering, ASCE, Vol. 110, No. 11, 1984.
- Briaud, J.-L., Tucker, L.M., Olsen, R.S., Pressuremeter, Cone Penetrometer and Foundation Design, Short Course Notes, Texas A&M University, 1985.
- Broms, B.B., "Lateral Resistance of Piles in Cohesionless Soils," Journal of the Geotechnical Engineering Division, ASCE, Vol. 90, No. SM3, 1964.
- Conroy, A.J., "Pile Load Tests at Lock and Dam 26 Replacement Project," Unpublished Paper, 19--.
- Coyle, H.M., Castello, R., "New Design Correlations for Piles in Sand," Journal of the Geotechnical Engineering Division, ASCE, Vol. 107, No. GT7, 1981.
- deRuiter, J., Beringen, F.L., "Pile Foundations for Large North Sea Structures," Marine Geotechnology, Vol. 3, No. 3, 1979.
- Fruco and Associates, "Overwater Steel H-Pile Driving and Testing Program," Report for Corps of Engineers, St. Louis, 1973.

Lowery, L.L., "TIDYWAVE Wave Equation Computer Program Utilization Manual." Pile Dynamics, Inc., Bryan, Texas, 1982.

Meyerhof, G.G., "Bearing Capacity and Settlement of Pile Foundations," Journal of the Geotechnical Engineering Division, ASCE, Vol. 102, No. GT3, 1976.

Peck, R.B., Hanson, W.E., Thornburn, T.H., Foundation Engineering, John Wiley and Sons, New York, 1974.

Reese, L.C., Cox, W.R., Koop, F.D., "Analysis of Laterally Loaded Piles in Sand," Sixth Offshore Technology Conference, Houston, 1974.

Schmertmann, J.H., "Guidelines for Cone Penetration Test Performance and Design," U.S. Dept. of Transportation, Report No. FHWA-TS-78-209, 1978.

Shihadeh, M.A., "Evaluation of In Situ Test Prediction Methods for Axially Loaded Piles at Lock & Dam 26 Replacement Project," Master of Engineering Report, Texas A&M University, 1987.